Dehazing with STRESS

Vincent WHANNOU de DRAVO

Department of Color Imaging

Gjovik University College

Professor Jon Yngve HARDEBERG

University of Saint-Etienne

Professor Alain TREMEAU

A thesis submitted for the degree of

To my sisters Myriam Gabriella Félicité, Michèle Misericorde, my brothers Benoit Guillaume, Jean, Macaire Romule and my father Urbain Henri.

Acknowledgements

I want to thank especially my tutors Prof. Jon Yngve HARDEBERG and Prof. Alain TRÉMEAU for their advices, patience, motivation, and immense knowledge.

I want to thank Prof. Ivar FARUP for introducing me the STRESS framework and Dr. Marius PEDERSEN the coordinator of my master programme in Norway for his suggestions at different moments of my work.

I would not have this good working atmosphere without people like Dr. Peter NUSSBAUM, Dr SUN, Yuan JIANGPING, and many others from The Norwegian Colour and Visual Computing Laboratory.

Dr. Arnt-Børre SALBERG for feedback from my report and my presentation at NOBIM.

I take this opportunity to convey my heartfelt gratitude to thank all my teachers from GUC and UJM.

I address many thanks to my lovely brothers and my mother: Hippolyte d'Assomption, Cécil Clément, Guenolé Pio and Marthe Sarah PADONOU.

I can't forget brother Christopher McKELVIE, Jessica EL KHOURY, Clément de DRAVO for reading some parts of my work and suggesting improvments.

Finally I would like to thank all the people who involved directly or indirectly in this work: Mohamed, Irina, Hemlig, Pablo, Jonas, Abdul, Rahif, Nicolas and Nicolas (the French), Yao, Christian, Dimitrius, Davide, my cousins, ...

Abstract

There exist today plenty of algorithms and many papers about dehazing or defogging, that is enhancing images taken in hazy or foggy conditions. To our knowledge none of them has got a significant result for dense and non-dense haze image at the same time. In this master thesis, we will propose an algorithm that are able to dehaze both dense and non-dense hazy images. Our hope comes from the fact that we observe in dense hazy images, the Spatio-Temporal Retinex-inspired with Stochastic Sampling (STRESS) framework (Kolås et al., JIST, 55(4), 2011) gives a more visually pleasing result when we compare it with the DCP algorithm (He et al., CVPR, 2009) for the same input. Our hypothesis is that STRESS uses one or more of its principles to enhance efficiently dense hazy images. In this work, we will show how we find out this hypothesis and also justify it.

For the purpose of our experiment, we define a new database where images are separeted according to their degree of haziness (fuzzy, medium and very fuzzy). The dehazing algorithms that we consider are typically (Fattal, Proc. ACM SIGGRAPH, 27(3), 2008), (Fattal, Proc. ACM SIGGRAPH, 34(1), 2014), To evaluate the quality of these dehazed images, we use some metrics and a psychophysical approach.

From this experiment on the previous works, we show their relationships with STRESS and finally the performance of the new algorithm which is the combination with some of them with STRESS idea is showed as well. Basically our algorithm assesses the hidden free-haze layer by assuming that there are three patterns almost in outdoor hazy images namely: sky region (or regions which have the same behaviour, like snow), far objects and near objects. The experiment shows also that our algorithm based on the two-scale STRESS approach, edge detection and Hidden Markov Model has often more visibility level than most of state-of-the-art algorithm when using the metrics defined in (Hautière et al., Image Analysis & Stereology Journal, 27(2), 2008). .

Keywords : STRESS framework based approach, image dehazing, contrast enhancement, haze physical model, algorithm design, performance evaluation, perception, psychophysical experiments

Additional keywords : Computer Graphics : image formation, Computer vision : depth estimation, Optimization problem : parameters estimation, Optics : light scattering, polarization

Contents

List of Figures

1 Introduction

1.1 Subject addressed by the master thesis

Nowadays, outdoor applications of media such as broadcasting winter sport events, camera monitoring, and driver assistance systems [Aponso and Krishnarajah, 2011] are often exposed to bad weather due to the presence of atmospheric particles [Narasimhan and Nayar, 2001] causing fog or haze. At the same time, fog or haze could have some benefits in the artistic domain [Ajaj et al., 2009; Gibson et al., 2013] through simulation or painting for instance. In [Narasimhan and Nayar, 2003], authors said that Leonardo Da Vinci's paintings, often contain an atmospheric perspective - known also as aerial perspective - of a background scene [26], where further scene points were painted brighter and bluer. The term aerial perspective was first employed by Leonardo Da Vinci [Britannica, 2015; Mencher, 2015] in his *Treatise on Painting*, in which he wrote: "Colours become weaker in proportion to their distance from the person who is looking at them.". Also called atmospheric perspective, aerial perspective is a method of creating the illusion of depth, or recession, in a painting or drawing by modulating color to simulate changes effected by the atmosphere on the colour of objects viewed from farther away. It is evident, then, that if painters use haze or fog to give the depth impression on their canvas, haze is quite important for one to perceive a scene as natural.

Here our goal for this work is not artistic, even if we would like to dehaze a hazy image without or with less artifacts. Our goal, in some way, is to have as an output, an artistic and realistic dehazed image. Haze, mist, fog, daze are static phenomena causing bad weather. That is why, it is quite important to enhance and/or restore images for these kind of applications [Yadav et al., 2014]. There are several classifications of fog removal in the literature. One possible classification in the field of haze removal shows two types of categories. The first is based on image processing and the second on a computer vision approach that uses a physical model [Wang and Xu, 2014] - or non physics-based methods vs. physic-based methods. We will present the relationship of the subject with computer graphics and optics, but the main approach adopted here will be based on computer-vision and spatial colour algorithms since we are dealing with STRESS.

In this thesis, our work will focus on the STRESS or Spatio-Temporal Retinex-inspired Envelope with Stochastic Sampling framework[1] [Kolås et al., 2011] - or ideas - and some state-of-the-art dehazing algorithms like the one developed by

[1] The concept is presented in Chapter 3.

[He et al., 2009] or the ones developed by Fattal [Fattal, 2008] and Fattal [Fattal, 2014]. Our goal is to show step by step how these algorithms work. And once this process is done, we will combine these dehazing algorithms with the STRESS framework in order to design a new dehazing algorithm for dense and non-dense hazy image. For each dehazing algorithm, we will completely demonstrate how it works and then make a comparison with a set of images that we take in Gjøvik, along with images from NRK and others from state-of-the-art dehazing papers. For the evaluation step, we will use a metric similar to the one developed in [Liu and Hardeberg, 2013] and also set-up also psychophysical experiments. The method presented in [Liu and Hardeberg, 2013] was first used in [Hautière et al., 2008]. For their approach, Hautière, Tarel, Aubert, and Dumont extract from both the image and its restored version, with visible edges; they then compute the ratio of the gradient of the visible edges between the two images. To demonstrate the enhancement of the visibility, they use a concept called *visibility level* developed by Adrian. Finally the computed level is used as an indicator of the visibility enhancement. In contrast, for the psychophysical experiments, a subjective approach is used and is based on the human visual judgement. The observers are asked to evaluate the enhancement quality by grading given hazy images dehazed by different algorithms against a set of dehazed images.

1.2 Problem Description

There exist today plenty of algorithms and many papers about dehazing or defogging - enhancing images taken in hazy or foggy conditions. To our knowledge none of them has yielded a significant result for both dense and non-dense haze[1] image at the same time. In this master thesis, we will try to solve this issue. Our expectation comes from our observations in dense hazy image, that the STRESS framework gives a more pleasing result when we compare it with [He et al., 2009] with the same input. For outdoor winter sports images (image from NRK) since they have a denser haze, we hope that the STRESS based dehazing algorithm will give us some interesting results or at least open the door to some interesting new investigations in the field.

Since the STRESS framework is not really designed for dehazing purpose, we need to find a way to adapt the algorithm in order to efficiently dehaze objects in the scene. In fact we observed for a given dense haze image that the haze on near objects is well removed by STRESS. So the challenge is to find a way to process distant objects (or sometimes middle objects) in the scene. The challenge will be to analyse state-of-the-art dehazing algorithms and to design a new algorithm based on the STRESS framework, by combining it with some ideas developed in

[1]The density factor of a haze is not clearly defined. In our case, we consider that a haze is dense when we could not get edge from objects in non-sky region. This assumption holds at almost all images in our database even if it could be false for objects like water or snow: the haze is not necessarily dense for these objects.

these previous dehazing papers.

1.3 Justification, Motivation and Benefits

The motivation for this present work stems from the observation that the proposed algorithms in the literature still have their limitations. Also no one of them in our knowledge has already approached dehazing based on the STRESS framework. For outdoor winter sports, most of the suggested dehazing algorithms fail because they require additional assumptions of the scene such as scene depth and multiple images; and suffer from less effective maintainence of colour fidelity [El Khoury et al., 2014]. Fog/haze/dust and mist could all influence the audience experience and become a challenge for broadcasting. Some of these dehazing algorithms take long time to process, and so a secondary challenge here is to find a good compromise between the image size and the processing time. The first challenge that we met for this master thesis, is obviously literature review. The reason is simply that the literature review requires knowledge of all the relevant papers within the scope of the thesis and how to well summarize what it has been covered within the scope of the subject. This is a difficult problem since one well known current issue in the research field is an explosion of information Major and Baden [2010].

1.4 Research Questions

- How to take into account the depth information in the STRESS algorithm in order to efficiently process far (and middle) objects - in the scene?
- What is a plausible prior about foggy scenes in order to process our images well?
- How can we use the physical model parameters and the STRESS framework to efficiently dehaze a hazy image?
- How are we going to evaluate the quality of the algorithms output?

1.5 Planned Contribution

In our master thesis, we are going to design a new dehazing algorithm based on the STRESS framework principle. We hope that our new algorithm will overcome the visibility issue in dense and non-dense hazy images. We will define a new database with our own hazy images and the one from NRK. Also the quality of our result will be evaluated by using the so-called visibility level and a subjective assessment.

1.6 The Background

Phenomena such as haze/ fog/ dust/ mist and cloud are technically classified as *aerosol* [Wikipedia, 2014]. According to [Wikipedia, 2014] *aerosol* is a colloid of fine solid particles or liquid droplets in air or another gas which can be natural or not. Fog and forest mist for instance are classified as natural phenomena whereas haze, dust or smoke are classified as artificial ones. These phenomena reducing visibility and causing bad weather differ mainly in the types and the sizes of the particles - see the table below - involved and their concentration in space [Narasimhan and Nayar, 2001].

Condition	Particle type	Radius	Concentration
Air	Molecule	10^{-4}	10^{19}
Haze	Aerosol	$10^{-2} - 1$	$10^{3} - 10$
Fog	Water droplet	$1 - 10$	$10^{-4} - 10$
Cloud	Water droplet	$1 - 10$	$300 - 10$
Rain	Water droplet	$10^{2} - 10^{4}$	$10^{-2} - 10^{-5}$

Table 1.1: Weather conditions and associated particles types, sizes and concentrations inspired from McCartney classification.

Therefore, solving the dehazing issue just by considering a single algorithm will be very difficult because there are so many parameters and some are unknown. In this report, cloud or rain are not processed here but fog, haze, mist. daze, dust and snow be considered and referred to as the same phenomenon. In other words, we will use the same model for all of these effects.

In order to better approximate a model for the subject we are dealing with, we should better understand the physics of the phenomena especially the optics involved (atmospheric optics, see [Narasimhan and Nayar, 2001]) because we are working with digital images. Remembering that our visual system and the camera which takes the haze images are very similar in term of optical model, understanding the haze issue under an optical approach will then help us to solve the problem in an efficient way. We can assume that the information coded in the picture and then our role would consist in decoding the information stored in the image. That means the optical model is the key to a better assessment of the solution. A similar point of view, is also developed by [Narasimhan and Nayar, 2001].

Efficiently solving the dehazing problem in digital images is challenging. The fact is that phenomena such as fog or haze lie in the crossroads of several disciplines: mathematics, chemistry, physics, biology; and environment. In other words, a natural model for haze is a massive and a very complex subject. This idea is underlined by [Zhang, 2010] where he says: “Aerosol also referred to as haze,

influence climate by absorbing and reflecting solar radiation and modifying cloud formation." and he added also "A better understanding of how aerosols form in the atmosphere could greatly improve climate models"; which means that all present aerosols models are just an approximation of the phenomena rather than actual models, and researchers are still investigating the field. Even if we just take into account the issue in the optics-related fields and minimize the others, fog, haze and mist are still very complex. In [Gutierrez et al., 2009], the idea of simplifying the task to the field of computer graphics and computer vision is supported by the authors who write: "existing algorithms still assume that light emitted by a source or reflected off a surface reached the sensor unaltered". In fact a direct consequence of the presence of such aerosols in the atmosphere is the scattering of light; sunlight specifically. Authors in [Gutierrez et al., 2009] claim that from a computer graphics side, the minimization or simplification of the problem is due mainly to the high complexity cost of simulating these phenomena while from a computer vision side, they are considered as "noise".

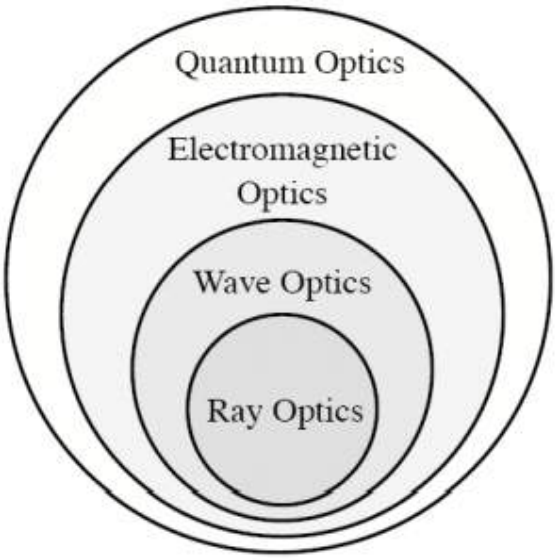

Figure 1.1: Light theory described by a series of increasingly complete optical models, where each successive model is able to account for more optical phenomena. In computer graphics, the simplest model, ray optics is often used [Gutierrez et al., 2009]

Before explaining the model that we are using here, we first must examine the optics of light.

1.6.1 Light

Light is defined by the Commission internationale de l'Eclairage (CIE) as electromagnetic radiation visible to the humain eye [CIE, 1987]. Its speed in vacuum is about 2.98^8 [Born and Wolf, 1999]. Other well known properties of light are its energy, its wavelength, its direction or polarization. Polarization is according to [Wikipedia, 2015b] a property of a wave such as light that can oscillate with more than one orientation. Since the report is related to the topic of fog or haze, the light that we refers to, is natural light [Hébert, 2013].

In [Glassner, 1989], Glassner writes that when a red photon and a green photon arrive at the eye simultaneously , the colour that perceived is yellow. This means that light is the main encoded information decoded by our eye in an image. Even if there is a relationship between light a physical quantity and colour, which is physiological sensation, it is worth noting that light and colour are two quite different concepts respectively related to the fields of optics and colorimetry[Hébert, 2013].

The model of light used in computer graphics is very near to the one used in optics with some simplications see [Gutierrez et al., 2009]. As previously noted, in computer graphics, a simple approach which takes into account ray optics and wave optics is already very expensive. In his course in computer graphics about ray tracing, [Fussell, 2010] supports simplifications of light models when he says in the field of geometrics optics: "modern theories of light treat it as both a wave and a particle. " Fussell then announces the geometric rule as follows:

- Light is a flow of photons with wavelengths. These flows are also called light rays.
- Light rays travel in straight lines in free space.
- Light rays do not interfere with each other as they cross.
- Light rays obey the laws of reflection and refraction.
- Light rays travel form the light sources to the eye, but the physics is invariant under path reversal (reciprocity).

Since we do not have anymore free space due to the presence of aerosol, the second rule above is broken and light is scattered. Light is not only scattered in atmosphere but also in solid heterogeneous media, such as paintings, papers, cotton and human tissues [Hébert, 2013; Sa, 1988].

Hence, instead of considering only one light ray for one point source, we can have one or multiple rays for one point source when they collide with these aerosol particules. In [Simonot et al., 2008], Simonot et al. and colleagues say that the reflectance of a thick particle medium depends on the optical properties of the binder as well as the optical properties, size, shape, relative locations, and concentration of the particles in the participating media. The effects of light scattering occur mostly in outdoor environments since they are caused by atmospheric

particles but they could happen or be simulated in indoor environments, for instance in a cave. According to [Wikipedia, 2015a], a theory that explains haze of fog phenomena well is the "Mie scattering theory" or the "Lorenz-Mie theory" [Mishchenko et al., 2005] derived from the Maxwell's equation. The Mie scattering model, by allowing for an explaination of the white color of cloud [Hébert, 2013], differs from the Rayleigh theory which allows the explaination of the blue colour of the sky. In fact, in Wikipedia [2015a], it is explained that the Rayleigh scattering model breaks down when particles size becomes larger than around 10% of the wavelength of the incident radiation. At that point, the Mie scattering model better approximates the phenomenon Wikipedia [2015a]. Due to the high number of parameters to consider, according to [Simonot et al., 2008], we can divide the main scattering model roughly into two main categories: (1) single scattering and (2) multiple scattering. Single scattering refers to a particle which scatters the light once.

1.6.2 Haze optical model

Before presenting the model used in this thesis to approximate phenomena such as haze and fog, we will first introduce image restoration concept. According to [Lagendijk and Biemond, 2000], the field of image restoration - sometimes referred to image deblurring or image deconvolution - is concerned with the reconstruction or estimation of an uncorrupted image from a blurred and noisy one. Essentially, it tries to perform an operation on the image that is the inverse of the imperfections in the image formation system. We will see that the haze model is an inverse ill-posed problem in the following lines and detail more in the Chapter 3. Image restoration algorithms distinguish themselves from image enhancement methods in that they are based on models for the degrading process and for producing the ideal image [Lagendijk and Biemond, 2000]. In this thesis since, we are using STRESS based algorithm and a physical model, we will use both enhancement and restoration method. In [Banham and Katsaggelos, 1997], the authors say that digital image restoration is a very broad field, as we are discussing, and thus contains many other successful approaches that have been developed from different perspectives, such as optics, astronomy, and medical imaging, just to name a few. In this thesis, we will take into account the haze optical model introduced by Koschmieder see [Koschmieder, 1924]. The physical model often used in dehazing paper has roughly two variants defined in the following equations:

$$I(x) \quad = \quad J(x)t(x) + (1-t)A(x) \tag{1.1}$$

where I is the observed image, J is the scene radiance, A the global atmospheric light and t the medium transmission. here too there are many approaches to solve this haze model. The goal here is to remove the fog by estimating, J, A and t. So we have three unknowns for one equation which means that the problem is

ill-posed. The above relationship is used for instance in [Fattal, 2008] and [He et al., 2009].

The second widely used formula or its variant is presented in [Narasimhan and Nayar, 2003] and a variant in [Tan, 2008] or [Tarel and Hautière, 2009]

$$E = I_\infty \rho e^{-\beta d} + (1 - e^{-\beta d}) I_\infty \tag{1.2}$$

where I_∞ represents the sky intensity and the term $e^{-\beta d}$ represents the tranmission with β being the scattering coefficient of the atmosphere; it represents the ability of a unit volume of atmosphere to scatter light in all directions and d, the depth of the scene point from the observer.

In the next Chapter, we will show step by step what is done before about solving the dehazing problem.

2 Related Work

2.1 Related Work

In this thesis, we are going to use the combination of a non-physics based approach (STRESS[1]) with a physics based approach. For this reason, our related work will be divided into two main groups. The first group will be those algorithms which based their analysis more on an image processing approach than a physics one. The second group will be the ones which worked directly with the physical model. That is precisely the point from which, today, we can say there exist three major types of dehazing algorithms:

- The first group is the image enhancement group algorithms, where the dehazing is done by using image enhancement techniques such as histogram equalization, homomorphic filter, wavelet transform, Retinex algorithms, luminance and contrast enhancement [Xie et al., 2010].
- The second group algorithms for dehazing purpose takes mainly into account a degradation model to remove haze from hazy images. Most of the algorithms of this group, considered as a state of the art for dehazing, used this approach due to the fact they take into consideration the haze physical model to restore the free-haze image. There are two main approches used for this second class for dehazing. The first approah is the stereo or the multi-views approach where the depth of the haze or other types of data are estimated by using two or more images [Kopf et al., 2008; Narasimhan and Nayar, 2001, 2003]. The other one uses a single image.
- The third group is the one which uses a combination between the first group and the second group. The work of Zhang et al. [2013] is an example of this class of algorithm.

Here, as we said previouly, we will take into account the second and the third groups simply because the first one does not really take into account the distribution of the haze in the image. Also in a certain sense our dehazing algorithm based on the STRESS framework can be classified as a part of the third group.

So let's start the review by the third group. Here we will relate three work at least for each category that we think very helpful for the research, we are doing

[1]We will see in the next chapter that STRESS is finally a hybrid method and also solves the haze physical model.

here.

2.1.1 Wang and Xu [2014] Method

One of the first interesting results from this class of dehazing algorithms is the work of [Wang and Xu, 2014]. They proposed to use mainly an image enhancement based approach by combining an adaptive Single Scale Retinex (SSR) with the dark channel prior developed by [He et al., 2009]. For each region or patch of the hazy image, they adapt the scale coefficient c of the SSR in order to efficiently remove the haze. To achieve this goal, they establish a relationship between the depth and the Retinex scale factor. The assumption is that in the haze images, the patch in which the far distant object are considered, look fuzzy and bleak which means that a small scale gauss filter will improve the quality of the patch or region better than a large one. In contrast to the patch or region where the near objects are considered, we have the inverse phenomenon [Tsutsui et al., 2012]. The idea of Wang and Xu is to process the patch according to the distance of the objects and adapt the scale Gauss filter in order to enhance efficiently the considered patch by taking into consideration the observation from [Tsutsui et al., 2012]. So the question now is how to get the depth map. For this step the authors take a part of the procedure of the algorithms of [He et al., 2009] which is the estimation of the transmission. In fact in the implementation of the dark channel prior of He and its colleagues, the transmission t(x,y) values are between 0 and 1 and represent how far the object in the considered patch is from the camera in some ways.

2.1.2 Zhang et al. [2013] method

The second work is [Zhang et al., 2013]. The algorithm used a physical model of haze mixed with a Retinex and an adaptive filter approach and works in three steps: the first step is the estimation of atmospheric light, then the transmission is estimated and finally the scene radiance is recovered. The first step is done by taking the 0.1% of brightest pixel in the dark channel. Then the pixels with highest value are selected to be the atmospheric light A such that:

$$A = \underset{0.1\%*h*w}{I(argmax(I^{dark}(x)))} \tag{2.1}$$

where I is the input and I^{dark} its dark channel, the computation used a 9×9 patch.

The second step of the algorithm is more tricky and needs more computations. Firstly, they introduce the brightness of an image as the mean of the image according to the 3 channels for a color image and corresponds to the brightness component of HIS (Hue - Saturation - Intensity) color space. We have then the

following formula:

$$I(x,y) = \frac{R(x,y)+G(x,y)+B(x,y)}{3} \tag{2.2}$$

The new image is then used to apply the method developed in [Elad, 2005] to get the Retinex. The method developed in [Elad, 2005] has the particularity of handling the illumination smoothness l and its proximity to s, while bounding it from above. The second part introduces the smoothness of the reflectance r, and requires to be close to the residual image $s-l$. Thus, noise can be discarded by becoming the residual $s-l-r$. By defining a novel Retinex algorithm, the output from the retinex step is called R'. From this, they define the anti-brightness image as:

$$I_{inv}(x,y) = D - R'(x,y) \tag{2.3}$$

where D is a constant fixed to 1.3 in the entire experiment. The transmission is then extracted from this anti-brightness image by applying an adaptative median filter. Finally the recovered scene is estimated by the following formula:

$$J(x,y) = \frac{I(x,y)-A(x,y)}{max(t(x,y),t_0)} + A(x,y) \tag{2.4}$$

where t_0 is fixed to 0.1. The output gives impressive result.

2.1.3 Xie et al. [2010] Method

Another algorithm that uses a similar principle is the work of [Xie et al., 2010] but instead of using the HIS color model as previously, they used the YC_bC_r (Y for luminance and two chrominance components C_b and C_r, representing respectively the blue-difference and red-difference chroma components) model for the transmission estimation step.

$$Y = 0,299 \cdot R + 0,587 \cdot G + 0,114 \cdot B \tag{2.5}$$
$$Cb = -0,1687 \cdot R - 0,3313 \cdot G + 0,5 \cdot B + 128 \tag{2.6}$$
$$Cr = 0,5 \cdot R - 0,4187 \cdot G - 0,0813 \cdot B + 128 \tag{2.7}$$

where (R,G,B) represent the red, the green and the blue component of a color image. Then they applied a multi-scale Retinex algorithm to the luminance component in order to obtain the transmission map. Once the transmission is obtained, the result is adjusted in such a way as in Zhang et al. [2013]. The airlight A estimation is done analogously as [He et al., 2009]. Now to recover the scene, they used the same formula as in [Zhang et al., 2013], We can also notice

the fact the work of [Xie et al., 2010] is done before the work of [Zhang et al., 2013] and the fact that both algorithms are quite similar.

2.1.4 Galdran et al. [2014] method

The dehazing algorithm developed by [Galdran et al., 2014] belongs also to the third group. In their work, Galdran and co-workers use for the image processing step, a spatial colour algorithm very similar to the Retinex called ACE (Automatic Color Equalization). The airlight and the transmission are roughly approximate. The typical value of the transmission chosen is $\frac{1}{2}$ and the airlight represents the max intensity value for each channel (very closed to the He et al. [2009] method). For the rest of the work, they used an iterative method which allow to control the degree of haziness by transforming the problem to an optimization problem - minimization. The energy function then corresponds to:

$$\begin{aligned} E(I^j) &= \frac{\alpha}{2}\sum_x (I^j(x) - \mu^j) + \frac{\beta}{2}\sum_x (I^j(x) - I_0^j(x))^2 \\ &\quad -\frac{\gamma}{2}\sum_x |I^j(x) - I^j(y)| \end{aligned} \tag{2.8}$$

where $j \in (R, G, B)$. To minimize the above equation, authors, first use the Euler-Lagrange derivative. The minimizer can be approximated by the following equation:

$$\delta E(I^j) = \alpha(I^j(x) - \mu^j) + \beta(I^j(x) - I_0^j(x)) - \gamma R(I^j(x)) \tag{2.9}$$

where the function $R(I)$ corresponds to the contrast enhancement operator:

$$R(I)(x) = \frac{\sum_y w(x,y)s(I(x) - I(y))}{\sum_y w(x,y)} \tag{2.10}$$

and s is a smooth approximation of the sign function, that accounts for the first derivative of the absolute value. Then they apply a gradient descent strategy. For this goal they pose $\frac{\delta I}{\delta t} = -\delta E(I)$ with t the evolution parameter. the final discretization in time corresponds to:

$$I_{k+1}^j = I_k^j(1 - \Delta t(\beta - \gamma)) + \Delta t(\beta\mu^j - \gamma I_0^j)) + \Delta t(\eta R(I_k^j)) \tag{2.11}$$

Now, we will present a method which restore the hazy image by using the haze physical model. For this part, we do not present in detail polarization based dehazing algorithm and other multiple images based dehazing algorithms

2.1.5 Fattal Approach

The second algorithm using single image dehazing is developed by Fattal. To overcome the dehazing task, Fattal makes the assumption that the shading and the transmission function are locally statistically incorrelated. The method is based on the physical model that we present in 1.6.2. The algorithm purpose is mainly to estimate the transmission. The airlight can be determined by taking the most haze-opaque pixel as first guess and can be refined later using the Lagrange-multipliers rule

$$\max_{A} \sum < A, v_1^i >^2 + < A, v_2^i >^2 \quad such \quad that \quad ||A||^2 = 1 \tag{2.12}$$

where A is a $3-$dimensional vector and v_1 and v_2 the two spanning components of a given region. To estimate the transmission, the assumption is that there is an additive noise ξ on the image. The transmission is then estimated in two ways. For the first way the error is not taken into account and for the second one, the error is estimated for each parameter introduced by Fattal. In fact with the first guess, we can compute $I_A(x)$, $I_{R'}(x)$ then $h(x)$ and η. Here is briefly the algorithm. Let us assume that the guess airlight is $A = (A_R, A_G, A_B)^T$ such that A_R. A_G, A_B are three scalars, then we can estimate $I_A(x)$ and $I_{R'}(x)$, so we have

$$I_A(x) \quad = \quad < I(x), A > ||A|| \tag{2.13}$$

and

$$I_{R'}(x) \quad = \quad \sqrt{||I(x)||^2 - I_A(x)^2} \tag{2.14}$$

Then we can compute $h(x)$ such that

$$h(x) \quad = \quad \frac{(||A|| - I_A(x))(x)}{I_{R'}(x)} \tag{2.15}$$

The corresponding η is:

$$\eta \quad = \quad \frac{C_\Omega(I_A, h)}{C_\Omega(I_{R'}, h)} \tag{2.16}$$

where

$$C_\Omega(I_A, h) \quad = \quad \frac{1}{|\Omega|} \sum_{x \in \Omega} (I_A(x) - E_\Omega(I_A(x))(h(x) - E_\Omega(h(x)) \tag{2.17}$$

and we have for a given function f, $E_\Omega(f) = \frac{1}{|\Omega|}\sum_{x\in\Omega} f(x)$ where $|\Omega|$ is the number of pixels in the patch. The quantity $C_\Omega(I_{R'}, h)$ is also computed in the same way. The first estimation of the transmission is then deduced using the relationship:

$$t(x) = 1 - \frac{I_A(x) - \eta I_{R'}(x)}{||A||} \tag{2.18}$$

After this point, the second estimation begins where ξ is inserted in the formula. Here also, a set B corresponding to the pixels which do not contain enough information is built by taking into consideration some constraints. Another transmission called $\hat{t}$ which excludes pixels from the set B is computed using a robust estimator different from the previous one defined in 2.17.

$$C_X(I_A, h) = \frac{1}{W_X}\sum_{y\in\Omega_x}(I_A(x) - E_X(I_A(x))(h(x) - E_X(h(x)) \tag{2.19}$$

so for a given function f, $E_X(f)$ is defined by $E_X(f) = \frac{1}{W_X}\sum_{y\in\Omega_x} f(x)w(x,y)$ where

y represents neighborhood pixels of the current pixel x,

$w(x,y) = exp(-d(\theta(x), \theta(y))^2/\sigma_\theta^2)$

$W_X = \sum_{y\in\Omega_x} w(x,y)$
By deducing σ_t from different steps:

$$P(t) \propto \Pi_{X\notin B} e^{-(t(x)-\hat{t}(x))^2/\sigma_t(x)^2} \Pi_{\forall x,y\in N_x} e^{-(t(x)-t(y))^2/(I_A(x)-I_A(y))^2/\sigma_s^2} \tag{2.20}$$

with $\sigma_s = 1/5$ then obtain the final t by solving $dlogP/dt = 0$, the scene is then recover by:

$$J(x) = \frac{I(x) - (1 - t(x) * A)}{t(x)} \tag{2.21}$$

Not long ago Fattal [2014] presented a dehazing algorithm based on the color-lines principle where he used a kind of decision graphs to discard pixel regions which are not candidate to satisfy his model. The basic idea of this new work is that the fog physical model could not be verified in all pixel and for those, they do not need to be taken into consideration in the processing.

2.1.6 Tan [2008] Approach

The physical model used by [Tan, 2008] is:
$I(x) = L_\infty \rho(x) e^{-\beta d(x)} + L_\infty (1 - e^{-\beta d(x)})$. Here are the steps of the algorithm

1. Estimate L_∞: This tridimensional vector can be estimated from pixels that have highest intensity from the input image

$$\begin{aligned} L_\infty &= (\max I_r, \max I_g, \max I_b)^T \\ &= (L_{\infty r}, L_{\infty g}, L_{\infty b})^T \end{aligned} \tag{2.22}$$

2. Compute α from L_∞:

$$\alpha_c = \frac{L_{\infty c}}{L_{\infty r} + L_{\infty g} + L_{\infty b}} \tag{2.23}$$

3. Remove the illumination color from I: Here a Retinex algorithm can be apply or any other color constancy algorithm or by using the relation 2.23. The resulting image is then called I'.
4. Compute the data terms $\phi(P_x|A_x)$ from I'
   $A \in [0, \sum_c L_{\infty c} - k]$ where $k = 20$. So for each value of A, compute
   - $|D\gamma'|^*_x$ such that

$$D(x)\gamma'(x) = (I'(x) - A(x)(1,1,1)^T) e^{\beta d(x)} \tag{2.24}$$

     where $I_c{}'(x) = \frac{I_c(x)}{\alpha_c}$ and $e^{\beta d(x)} = \frac{\sum_c L_{\infty c}}{\sum L_{\infty c} - A(x)}$

   - $\phi(P_x|A^*_x) = \frac{C_{edge}([D\gamma']^*)}{m}$ where m is the normalized factor and takes into account the patch size and such that:

     $C_{edge}([D\gamma']^*_x = \frac{\sum_c L_{\infty c}}{\sum L_{\infty c} - A} \sum_{x,c} |I_{x,c}{}' - I_{x-1,c}{}'|$
     The index $(x-1)$ represents neighborhood pixel of the current pixel x.
5. Compute the smoothness term $\psi(A_x, A_y)$,
   $\psi(A_x, A_y) = 1 - \frac{A_x - A_y}{\sum_c L_{\infty c}}$ and A_y is the smoothness term
6. Compute the inference which yields the airlight So here we consider the Markov Random Field (MRF) as

$$E(A_x|P_x) = \sum_x \phi(P_x|A_x) + \eta \sum_{x,y \in N_x} \psi(A_x, A_y) \tag{2.25}$$

   η is the strength of the smoothness term and N_x represents the set of neigh-

borhood pixels, so at the end of day, we will get the estimation of $A(x)$

7. we can then recover the scene by using the relation 2.24.

2.1.7 He et al. [2009] Approach

The model used by [He et al., 2009] is the one described above in 1.1, the data-structure uses here for the component A is different from the one used in Fattal approach. For this method A is a $M \times N$ matrix. The [He et al., 2009] dehazing algorithm is based on the Dark Channel Prior (DCP or DC). The DCP is a concept introduced by He et al. during his thesis [He, 2011] and based on a statistic observation of hazy outdoor image. The concept states that most local patches in haze-free outdoor images contain some pixels which have very low intensities in at least one color channel. By using this assumption, they estimate the unknown parameters in the haze physical model. The formal definition of the concept of DCP for a haze-free image J is:

$$J^{dark}(x) = \min_{c}(\min_{y \in \Omega(x)}(J^{c}(y))) \tag{2.26}$$

Where J^c is a color channel of J and $\omega(x)$ is a local patch centered at x. [He et al., 2009] observe that in non-sky region the dark channel of the haze-free image is low and very near to the null pixel value. Also they notice the fact the dark channel is a rough approximation of the thickness of the scene.

According to the authors, the dark channel, the low intensities in the dark channel is due to 3 factors:

1. Shadow for instance the shadow of cars, building.
2. The colorful object of surface for example green grass, tree or plant.
3. dark objects or surfaces like dark tree, trunk and stone.

Below the algorithm is described.

Algorithm: Single image haze removal algorithm based on the dark channel prior

1. Estimate the atmospheric light A as described below
2. Estimate the transmission by:

$$\tilde{t}(x) = 1 - w \times \min_{c}(\min_{y \in \Omega(x)}(\frac{I^{c}(y)}{A^{c}})) \tag{2.27}$$

where $\tilde{t}$ is the patch transmission and w a weight

3. Define the transmission by soft matting i.e solve the linear equation for t

$$(L + \lambda U) \quad = \quad \lambda \tilde{t} \tag{2.28}$$

4. Recover the scene radiance J by:

$$\min_{y \in \Omega(x)} (I^c(y)) \quad = \quad \tilde{t}(x)(\min_{y \in \Omega(x)} (J^c(y))) + (1 - \tilde{t}(x))A^c \tag{2.29}$$

Here is explained how each step of the algorithm is done:

1. To estimate the atmospheric light, they pick 0.1% of the brightest pixel in the dark channel pixels, then the pixel which have the highest value of choosen dark channel well approximate the atmospheric light.
2. To estimate the transmission, they proceed as follows. First they apply the min operator on each color channel by using the definition of haze physical model and by assuming $\tilde{t}$ constant in a local patch:

$$\min_{y \in \Omega(x)} (I^c(y)) \quad = \quad \tilde{t}(x)(\min_{y \in \Omega(x)} (J^c(y))) + (1 - \tilde{t}(x))A^c \tag{2.30}$$

   Since the airlight contain the highest pixels values, by applying the min operator over the 3 channels, they obtain:

$$\min_c(\min_{y \in \Omega(x)} (\frac{I^c(y)}{A^c})) \quad = \quad \tilde{t}(x) \min_c(\min_{y \in \Omega(x)} (\frac{J^c(y)}{A^c})) + (1 - \tilde{t}(x)) \tag{2.31}$$

   By using the property of the dark channel on haze-free image:

$$J^{dark}(x) \quad = \quad \min_c(\min_{y \in \Omega(x)} (J^c(y))) = 0 \tag{2.32}$$

   which means that the patch transmission can be written now as follows:

$$\tilde{t}(x) \quad = \quad 1 - min(min(\frac{I^c(y)}{A^c})) \tag{2.33}$$

   Remember the aerial perspective described in the introduction. So to keep a small amount of the haze. The transmission patch is finally defined in the equation 2.27. Here $w = 0.95$ is assigned as the small amount of haze, allowing the aerial perspective.
3. For the transmission refining part, the equation 2.28 is solved by using the soft matting approach. The technique is well defined in [Levin et al., 2008].

4. The last point of the algorithm is just an application of the formula once the two parameters allowing the recovering of the scene radiance J, are estimated.

2.1.8 Tarel and Hautière [2009] Approach

The method developed by Tarel and Hautière used the model described in [Tarel and Hautière, 2009] whose a variant can be seen in 1.2.Then they pose the atmospheric veil $V(x,y) = I_S(1 - e^{-kd(x,y)})$.

$$I(x,y) \quad = \quad R(x,y)(1 - \frac{V(x,y)}{I_s}) + V(x,y) \tag{2.34}$$

where $I(x,y)$ is the observed image intensity (gray or RGB) at pixel(x,y) and $R(x,y)$ is the haze-free image. With this new formulation, the problem consists of infering the atmospheric veil in order to dehaze. The first assumption for this algorithm is that we have white balance prior to visibility restauration. Meaning that I_S can be set at $(1,1,1)^T$ and $I(x,y)$ is normalized between 0 and 1.The other constraints are that $V(x,y)$ is positive and $V(x,y) \leq W(x,y)$ where $W(x,y) = \min I(x,y)$. The problem can be summarized to solving the following optimization problem:

$$\text{argmax} \int_{x,y} V(x,y) - \lambda\Phi(||\bigtriangledown V(x,y)^2||) \tag{2.35}$$

such that $o \leq V(x,y) \leq W(x,y)$. Due to the high cost of this optimization problem, the value of V should be estimated by using a less computational approach. In their paper, the authors translate the above optimized solution into a percentage of the difference between local average of $W(x,y)$ and its standard deviation. So to estimate the veil, other quantities are needed:

$A(x,y) = \text{median}_{S_v} W(x,y)$ and

$B(x,y = A(x,y) - \text{median}_{S_v}(|W - A|)(x,y))$

Finally the computation of $V(x,y)$ is defined by

$$V(x,y) \quad = \quad \max(\min(pB(x,y), W(x,y)), 0) \tag{2.36}$$

and $p = 0.95$

Using just the median introduced some artifact, so instead they used the median of median along lines. For each pixel, the operator centers the segment of size S_v on the current pixel. The median value along S_i is computed and saved

as m_i. The collected m_i for the current pixel along the whole centered segments are filtered by taking the median value of m_i such that $1 \leq i \leq n_v$ allowing the edges preservation. The recovered is then difined as:

$$R(x,y) = \frac{I(x,y) - V(x,y)}{1 - \frac{V(x,y)}{I_S}} \tag{2.37}$$

Finally a gamma correction and a tone mapping are applied to the restored image.

2.1.9 Gibson et al. [2013] Approach

In their paper [Gibson et al., 2012], Gibson and its co-authors used a method which can be seen as a variant of the approach developed earlier by [He et al., 2009]. The novelty of their algorithm can be seen through the definition of the concept of the Median Dark Channel Prior (MDCP). The formal definition of MDCP is:

$$\Theta_M(m,n) = \underset{k,l \in \Omega(m,n)}{median} \left(\min_{c \in (r,g,b)} \frac{\hat{x}(k,l,c)}{a(c)} \right) \tag{2.38}$$

Where a represents the coefficients of airlight, $\hat{x}(k,l,c)$ a pixel value on a specific channel.

Other versions of the dehazing process were developed by Gibson.

In [Gibson and Nguyen, 2011], Gibson and Nguyen show the geometrical meaning of the Dark Channel Prior (DCP), by observing that the DCP is equivalent to the Löwner-John ellipsoid either from R-G, G-B or R-B planes.

In [Gibson and Nguyen, 2013a], authors effectively used the color ellipsoid prior derived from the DCP for the dehazing task.

Finally in [Gibson and Nguyen, 2013b], they use a locally adaptive Wiener filter, to speed up the fog removal process.

2.1.10 Kratz and Nishino [2009] and Nishino et al. [2012] Methods

These works share some similitude, the main idea is to solve these two problems by using a Hidden Markov Model (HMM). Two hidden layers are then considered in order to achieve the dehazing task namely the scene albedo term and the depth.

2.1.11 other approaches

Oakley and Bu [2007] use the statistic of images containing fog or mist to estimate the airlight and from that point derive the defogging algorithm using Monte Carlo approach on synthetic images.

In [Jr., 1988], Jr. use a wavelet based decomposition of an image for the detection and removal of haze.

Carr and Hartley [2009] adopt the benefit of priors relative to the scene ge-

ometry and an alpha-expansion optimization in order to estimate reliably the fog equation parameters.

Matlin and Milanfar [2012] endorse a physical model of fog which takes into consideration the noise. The fog removing assignment is then done with two methods by combining the denoising and the defogging process. The first using the BM3D algorithm[Dabov et al., 2007], the second an iterative non-parametric regression.

Schechner et al. [2001] use a physical model in which, there are two unknowns: The scene radiance in the absence of haze and the airlight parameter. To solve their equation, authors use two images or more, taken under different polarization conditions.

Shwartz et al. [2006] use a rough prior which state there is a statistical independence between the airlight and the transmission component and solve the haze physical model by using a polarization based approach.

Narasimhan and Nayar [2001] make an estimation of the airlight and the direct transmission thanks to two or more images under different unknown weather condition.

Narasimhan and Nayar [2003] used another approach for the dehazing question which consists to using of a single image as input and take into account interaction with an user to solve ambiguity of the physics-based equation.

[bing Zhu et al., 2014] make an improvement of DCP by taking into consideration sky and non-sky region to avoid saturation effect.

Short while ago, [Dou et al., 2015] introduce a new dehazing algorithm where they alternate the combination of a Laplacian regularization with the Beltrami framework. In their approach, they estimate iteratively first the airlight, then the transmission and finally the radiance of the scene.

Fan et al. [2015] recently come out with an approach which explicitly formulates aerial perspective in human perception and using the DCP for estimating the transmission. They also use for this estimation the maximum visibility as a parameter. Finally they use some metrics in order to evaluate their results with some of the state of art method. This kind of evaluation is also presented in the defogging method review by [Liu and Hardeberg, 2013].

3 STRESS and the Dehazing Task

In this chapter, we are going to present the theoretical part of our work. Sometimes, we will make some quick experiment to investigate or prove a particular point. It is worth noticing that the problem, we are going to solve here, based on the Koschmieder [1924] law is an inverse ill-posed problem. We will first present what we mean by inverse ill-posed problem. Then we will introduce the STRESS framework.

3.1 Inverse ill-posed Problem

The Equation 1.1 expresses the forward representation of an inverse ill-posed problem, since the only I parameter is available and the other in the right hand side is not as we already said in the previous chapter. This ill-posedness (ambiguity) is due to the fact that the Equation 1.1 does not have a single solution but has many solutions or even no solution. The only way to solve this kind of problem is to guess the solution. The general expression of this kind of problem can be written as the following:

$$y = f(x) \tag{3.1}$$

In a mathematical point of view, $f : X \mapsto Y$ where X and Y are two sets, is called a function or a model. The task of inferring[1] or computing the parameter y from x is known as a forward problem and is an easy problem, since the function f is explicitly known and x given[Fieguth, 2011, chap. 2]. The task of inferring the reverse procedure is known as an inverse problem and is a hard problem. The problem is hard for two main reasons: The function f^{-1} is not often known in its explicit form or f^{-1} does not even exist. According to Fieguth [2011]; Hadamard [1923], a well-posed problem should fulfil three criteria:

- Existence: $\forall y, \exists x, y = f(x)$ which means that for every measurement or observation or data y, there exists at least a corresponding x. This condition can sometimes correspond to the subjectivity principle, that is also $f(f^{-1}(Y)) = Y$.
- Uniqueness: $\forall y, \exists ! \, x, y = f(x)$ which can be translated as for every measurement y, there exists one and only one corresponding x. This property can

[1] the task of inferring a model is a subset of more general problem called identification system [Ljung, 1999]. We will talk a bit more about this in the appendix A.

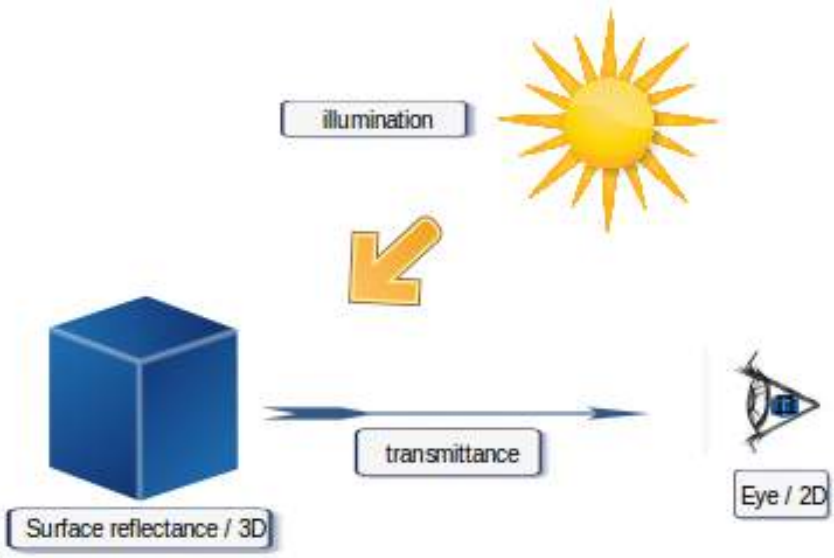

Figure 3.2: Basic factor involving in human vision. These factors can be related for instance in geometry sense, motion, colour etc.

refer sometimes to the injectivity principle, that is $\forall(x_1, x_2) \in X^2, x_1 \neq x_2 \Rightarrow f(x_1) \neq f(x_2)$.

- Continuity or stability: x depends on y in a continuous way

Any equation for which one or more of these three conditions is not satisfied, is an ill-posed or an improperly-posed problem [Kirsch, 1996].

The stability or the continuity is the most important point since we do not have any solution to our inverse problem or many solutions (an infinite solutions in worse case). In fact the stability principle will help us to be close as much as possible to one of solutions to the problem. We can write this continuity principle mathematically as the following:
$c \in X, \forall\epsilon > 0, \exists\sigma > 0; \forall x \in X$

$$|x - c| < \sigma \Rightarrow |f(x) - f(c)| < \epsilon \tag{3.2}$$

More intuitively, we can say that if we want to get all the f(x) values to stay in some small neighborhood around f(c), we simply need to choose a neighborhood which should be small enough for the x values around c, and then we can do that no matter how small the f(x) neighborhood is [Wikipedia, 2015c]. In other words, we can find an approximation of the solution. From that point, a question could be how to find a good solution near to the one we are looking for? The answer can be inference: if we know how the solution looks like, we can use this prior to

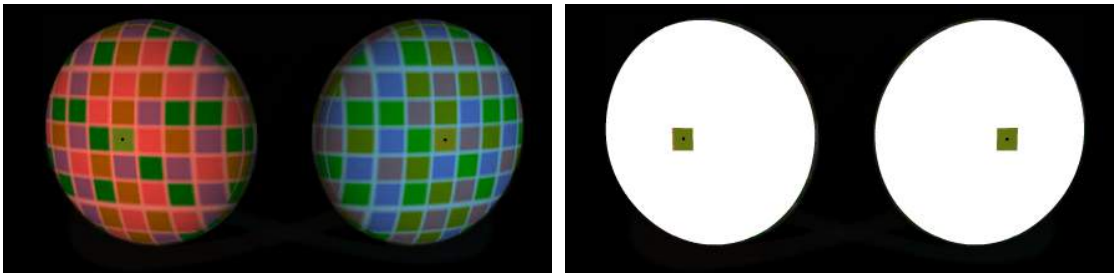

Figure 3.3: Basic factor involving in human vision. This example is related to the colour. On left two different illuminants are illuminating a same object. The colour of the neighborhood of a choosen pixel (see right picture) does not look the same under these two illuminants (see left picture).

infer our model. Before developing this point, let's talk a little bit about inverse problem in vision.

It is now well accepted that human beings have a complex vision system, which cannot be modelled completely in an objective way. Four factors involve in human perception: light source, reflectance, transmittance and eyes (see Figure 3.2). The brain can also be added to the list, since from the eyes, some information are sent to the brain for other processings. There exist many inverse problems in vision: one can be related to the geometry, the motion, the color, etc. In geometry sense for example, the 3D object in the scene is transformed in the eyes as a 2D object. In that particular case, the ill-posedness is due to the lack of matching between the 3D representation and its 2D image.

As we can see on Figure 3.3, we have a strange way to perceive colour. Just by changing the illuminant colour, the environment colour of a given pixel do not look the same anymore. The right colour informations are still in the data, and our eyes, guided by our brain, can perceive the true colour but this kind of operation is still a puzzle in the field of digital image processing [Khan et al., 2013]. This phenomenon is also governed by an inverse ill-posed problem. The good news about our current problem (the dehazing task) using the STRESS framework is that STRESS also solves an ill-posed problem. The question now is that the solution given by STRESS is still related to the dehazing task? Should we be able to adapt this model to the dehazing task or should we need to build a completely new approach (which would not depend on the STRESS framework)? Before answering these questions, we will first in the next section, present the STRESS framework.

3.2 The STRESS framework

The STRESS (Spatio-Temporal Retinex-inspired with Stochastic Sampling) framework is first introduced by Kolås, Farup, and Rizzi in [Kolås et al., 2011]. The STRESS framework has many applications as we can see in [Kolås et al., 2011], [Islam and Farup, 2011] and [Simone and Farup, 2012]. Here we are mostly interested in constrasting the enhancement of the image, by doing so, we will deal with the stretching part of this framework. STRESS is an automatic color adjustement algorithm in the same way as color constancy algorithms like Retinex or ACE. The STRESS framework is derived from these two previous work: [Shaked and Keshet, 2002] and [Provenzi et al., 2007]. STRESS borrows from [Shaked and Keshet, 2002], the idea of envelope but instead of using one envelope, two envelopes E^{min} and E^{max} representing two signals, are used. From [Provenzi et al., 2007], the random spray technique is mimicked. The spray is a kind of circular patch centered at the current pixel p_0, in which the samples p_i ($\neq p_0$) are taken in order to reconstruct the initial signal. For a given iteration, all the samples are different from each other. The framework is based on the locality and globality principle which means that a given sample candidate can represent either local or global minimum/maximum depending of three main parameters namely:

1. n_i or N the number of iterations
2. n_s or M the number of samples
3. R the radius of the spray

As we will see soon, these three parameters are very important in the dehazing task. Now let's describe the STRESS framework a little bit more in detail.

The framework processes each pixel p_0 the same way. For each pixel p_0 and for each single iteration (until the N^{th}), M samples are randomly selected from the spray of radius R centered at p_0. If a chosen sample is outside the image, the rule will be to try until a sample is found within the image. The envelopes are constructed in such away that locally $E^{min} \leq p_0 \leq E^{max}$. Here are the definitions

of these two envelopes as described in [Kolås et al., 2011].

$$E^{min} = p_0 - \bar{v}\bar{r} \tag{3.3}$$
$$E^{max} = p_0 + (1-\bar{v})\bar{r} = E^{min} + \bar{r} \tag{3.4}$$
$$\bar{r} = \frac{1}{N}\sum_{i=1}^{N} r_i \tag{3.5}$$
$$\bar{v} = \frac{1}{N}\sum_{i=1}^{N} v_i \tag{3.6}$$
$$r_i = s_i^{max} - s_i^{min} \tag{3.7}$$
$$v_i = \begin{cases} 1/2 & \text{if} \quad r_i = 0, \\ (p_0 - s_i^{min})/r_i & else \end{cases} \tag{3.8}$$
$$s_i^{max} = \max_{j\in\{0\ldots M\}} p_j \tag{3.9}$$
$$s_i^{min} = \min_{j\in\{0\ldots M\}} p_j \tag{3.10}$$

From Equations 3.9 and 3.10, the maximum and the minimum of a set of M samples are computed. From these points, v_i , the relative value of the center and the averaging ranges r_i are computed in Equations 3.8 and 3.7. From these equations, are computed over all iterations the average of the previous quantities in Equations 3.5 and 3.5. Finally the value of the two envelopes E^{min} and E^{max} are deduced in 3.4 and 3.3.

It is also worth remembering that STRESS is a solution to an inverse problem. The backward model of this inverse problem is derived from the Retinex model presented in [Provenzi et al., 2007] as the following:

$$L(i) = I(i)\frac{1}{N}\sum_{k=1}^{N}\frac{1}{I(x_{H_k})} \tag{3.11}$$

In this expression x_{H_k} stands for the highest pixel intensity value, L the (normalized) lightness factor and N the collection of paths.The goal of the STRESS framework is to assess the unknown lightness L.

As we say in Chapter 2, the haze model solution also estimates the real radiance of the scene quite differently in comparison to the Retinex model initiated from [Provenzi et al., 2007]. In other words the model defined in Equation 1.1 and the one defined in Equation 3.11 are not similar in the way they have been expressed and the parameters do not represent the same quantities. However we can see now that the two models solve both an inverse ill-posed problem by using a

probabilistic approach. In the case of the state of the art algorithms, an iterative Bayesian approach is often used by assuming some priors and for STRESS, an iterative stochastic approach by observing the locality and the globality principle.

Here we should be noticing that at the beginning of this project we observe that STRESS gives us a really pleasing image when we have a really dense haze compared to the state of the art algorithms as in the work of [He et al., 2009] or [Gibson et al., 2013]. An example is given on Figure 3.4

(a) Original (b) DCP (c) STRESS

Figure 3.4: Image taken in Gjøvik (Norway) - Lac Mjøsa - at the beginning of the winter 2014-2015. As we can see, the fog on near objects is well removed, far objects still have fog and we do not obtain a saturation effect with (c), that we have in the case of (b).

From that point of view, the first idea which comes to our mind reads: if that STRESS[1] is visually able to give the same visibility with for instance [He et al., 2009] for the particular case of dense haze and without any saturation effect, then maybe it is possible to use STRESS for any other case of haze since we know that a dense haze is a critical case of haze. Another one is why STRESS is removing haze just for near objects? And so on. In the next Section we will show that the homogeneous haze should be taken into account if we want to know about STRESS and the dehazing task.

3.2.1 Artificial Homogeneous Haze

As we explain in the previous section, the STRESS framework treats each pixel in the same way. We are now making the assumption that if STRESS can dehaze any hazy image, it can surely dehaze a homogeneous haze too. Therefore the test which comes to our mind is to simulate an artificial homogeneous haze on natural images and then process the synthesized images with STRESS. If STRESS works as expected, we should get a good removing of fog from this processing.

[1]The experiment is also made with other spatial color algorithms like Retinex or ACE. The results show that ACE is also interesting for the dehazing task since we have visually pleasing output as we will show in the next Chapter. At the same time, some authors as we show in the previous Chapter have already explored the dehazing problem based on ACE.

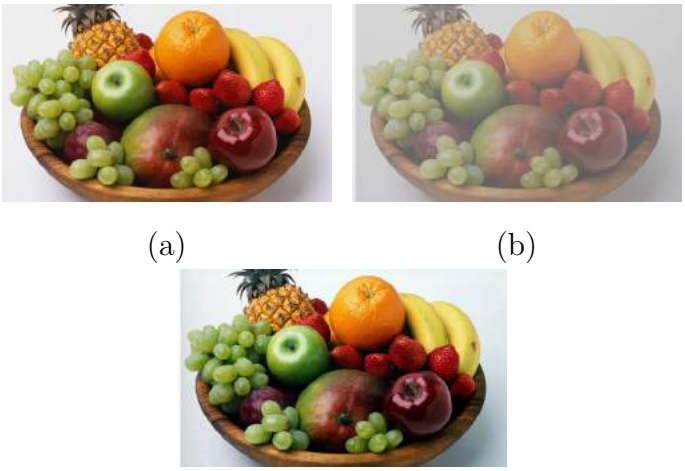

(a) (b)

(c)

Figure 3.5: (a) the original image, (b) the synthesized homogeneous fog, (c) the haze-free using STRESS with $n_i = 100$ and $n_s = 15$. For this experiment, with homogeneous fog, we notice that by taking more samples, the output of STRESS get close with the original image visually. Original taken from www.theguardian.com

We choose 10 natural[1] images on the internet and we apply a thin layer on them with a different density to simulate the (dense) homogeneous haze on them. we make some quick visual experiments to measure the visibility level on these output image. The experiment shows that STRESS dehaze quite well the images as you can see on Table 3.2.

Also visually, it's trivial that the haze is removed from these images, an example is given in Figure 3.5.

With this experiment, we can see how well STRESS dehaze the hazy images. Now the question could be: is STRESS solving the removing fog problem randomly or is there any relationship between the haze physical model and the STRESS framework? We can also try to know if the result that we get experimentally with dense and homogeneous haze is just random process or not. We will see soon the answer is that the process is not completely a random process. Therefore make sense to have got the result that we have already obtained with the dense and homegeneous haze.

Here is the meaning of each variable in the Table 3.2 taken from [Hautière et al., 2008]:

$$e = \frac{n_r - n_0}{n_0} \tag{3.12}$$

[1] images which do not contain haze

Synthesized (b) vs.	e	$\bar{\gamma}$	σ
(a)	1.04	2.12	0.33
(c)	1.71	2.40	0.86

Table 3.2: Corresponding to Figure 3.5
The high value of the parameter e with image (c) compared to image (a) prove that we have more edges in (c) using STRESS than original one (a).

In Equation 3.12 n_0 (respectively n_s) coincides with the cardinal numbers of set of visible edges in the original image (respectively in the restored image). e The rate of new visible edges in the contrast restored image I_r - vs I_o the original image. The value of e allows to assess the ability of the method to restore edges which were not visible in I_o but are in I_r.

$\bar{\gamma}$ stands for the geometric meaning of the ratio VL defined below:

$$\gamma = \frac{VL_r}{VL_0} \tag{3.13}$$

In Equation 3.15, VL represents the visibility level and is defined as follows:

$$VL = \frac{(\Delta L/L_b)_{actual}}{(\Delta L/L_b)_{threshold}} \tag{3.14}$$

In 3.14 ΔL is the difference between target and background and L_b is the luminance of the background.

$$\sigma = \frac{n_s}{dim_x * dim_y} \tag{3.15}$$

Above n_s is the number of pixels which are saturated (black or white) after applying the contrast restoration but were not before.

dim_x and dim_y represent respectively the width and the height of the image.

3.2.2 The Model of Haze that STRESS approximates

After experimenting with the STRESS framework by manipulating different parameters especially the number of iterations and the number of samples on synthesized haze, we notice experimentally that the output get close to the original image by increasing the number of samples and the haze are well removed, as you can see on Figure 3.5.

The idea originates from these previous experiments which prove that there

might be a link between the STRESS model and the haze physical model. To check this hypothesis, we will check the STRESS output with the envelope values. And that makes sense, because we know from [Kolås et al., 2011] that the STRESS output can be expressed by:

$$P_{STRESS} = \frac{P_0 - E^{min}}{E^{max} - E^{min}} \tag{3.16}$$

In other words P_{STRESS} is a stretching between E^{min} and E^{max} and its values is obviously between 0 and 1.

In the work of [Tan, 2008] as shown on previous chapter by the Equation 1.2, the haze model is a bit different from the one in 1.1. We repeat this physical equation here as follows:

$$E = I_\infty \rho e^{-\beta d} + (1 - e^{-\beta d}) I_\infty$$

the variable meaning is presenting as the following, I_∞ represents the sky intensity and the term $e^{-\beta d}$ represents the transmission with β being the scattering coefficient of the atmosphere; it represents the ability of a unit volume of atmosphere to scatter light in all directions and d, the depth of the scene point from the observer.

According to the formula above and by doing some variables changing, we can rewrite the model as follows:

$$I(x) = J(x)t_1(x) + (1 - t_2(x))A(x) \tag{3.17}$$

Theorem 3.2.1. *The minimum envelope E^{min} in the STRESS framework solves the haze physical model defined in Equation 3.17.*

Proof. The multiplicative factor t on the right-hand side in the Equation 1.1 is replaced in the above formula by t_1 and t_2. So now let's consider that the new haze model is expressed by the Equation 3.17. By considering the two definitions of the envelopes E^{max} and E^{min}, we can write:

$$p_0 = E^{max} - (1 - \bar{v})\bar{r} \tag{3.18}$$

$$p_0 = E^{min} + \bar{r} - (1 - \bar{v})\bar{r}$$

$$p_0 = E^{min} + [1 - (1 - \bar{v})]\bar{r} \tag{3.19}$$

From 3.19, we can find $\bar{w} \in [0, 1]$ such that $\bar{w} = 1 - \bar{v}$ since we know that $\bar{v}$ or $\bar{r}$ are elements of $[0, 1]$ from [Kolås et al., 2011]. . We can then write 3.19 as the

following:

$$p_0 = E^{min} + (1 - \bar{w})\bar{r} \tag{3.20}$$

Let us pose now $\bar{w_1} = 1$ and $\bar{w_2} = \bar{w}$. So the above relationship can then be written:

$$p_0 = E^{min}\bar{w_1} + (1 - \bar{w_2})\bar{r} \tag{3.21}$$

In our case E^{min} concords with the radiance J and p_0 to the input pixel value. We can therefore see the link between the Equation 3.21 above and the Equation 3.17. Also from [He et al., 2009], it is said that the transmission $t \approx 0$ for distant object. And from [Fattal, 2014], we know that a good estimation of the transmission parameter should be such that $t \in [0, 1]$, which obviously is the case for our two pseudo-transmissions $\bar{w_1}$ and $\bar{w_2}$ here. At the same time, we can notice that the first transmission term $\bar{w_1}$ does not take into account the distant object since its value is fixed at 1. The second transmission term $\bar{w_2}$ may take into account the distant object. In fact it represents the complementary of $\bar{v}$ in the interval $[0, 1]$. □

Model Validation. *If we approximate*[1] p_{STRESS} *in Equation 3.20 by* E^{min}*, then* p_{STRESS} *is also solving the same haze physical model. Since we know that* $p_{STRESS} \in [0, 1]$*, then by normalizing its final expression in Equation 3.21, we come back again on the initial definition of* p_{STRESS} *in (3.16).*

Remark. *In the following, a given variable* v *will be said low, when there exists* $\epsilon_0 \in [0, \frac{1}{2}[$ *such that* $v < \epsilon_0$*. A given variable* v *will be said high, if there exists* $\epsilon_1 \in]\frac{1}{2}, 1]$ *such that* $v > \epsilon_1$*. Also, we will implicitly or explicitly admit the validity of the DCP for near objects and far objects.*

Corollary 3.2.1.1. *If* p_0 *is low then* p_{STRESS} *solves the physical model defined in Theorem 3.2.1.*

Proof. From [Kolås et al., 2011], we know that $p_0 = E^{max}$ at the global maximum and $p_0 = E^{min}$ at the global minimum. So $E^{max} \in [0, 1]$ and $E^{min} \in [0, 1]$ since p_0 is normalized in $[0, 1]$. If p_0 is low then p_{STRESS} will behave as E^{min} since p_{STRESS} is a stretching of p_0 betweeen E^{min} and E^{max} □

Another parameter which plays a great role in the removing of the fog especially for near objects in this Section is the radius parameter R fixed such that $R = max(image_{width}, image_{height}) = \max(w, h)$. This kind of sampling with

[1] This validation takes also into account, what we prove theoretically and empirically in the following lines.

$R = \max(w, h)$ can be compared to the randomized global sampling method described in [He et al., 2011] in some way.

Let's see now the impact that this parameter has on the dehazing task. We know from [Kolås et al., 2011] that the parameter $\bar{v}$ represents the average of v_i such that:

$$v_i = \begin{cases} 1/2 & \text{if} \quad r_i = 0, \\ (p_0 - s_i^{min})/r_i & else \end{cases}$$

Proposition 3.2.2. *Setting the radius parameter R in the STRESS framework for the dehazing task, such that $R = \max(w, h)$ allows to remove fog from near objects at least.*

Proof. Thanks to Theorem 3.2.1, we just need to show here the transmission $\bar{w}_2$ is high. Since $R = \max(w, h)$, almost all the pixels except p_0 are candidates for the sampling step.

The case where, roughly all $v_i = \frac{1}{2}$ is not very interesting, because we know that means objects in the middle of our image will be dehazed according to what we said previously and also the radius R for that particular case has no direct effect on $\bar{w}_2$. Let see now the other case. Since we know $R = \max(w, h)$, we can say that s_i^{max} and s_i^{min} represent enough well the max sample and the min sample, which means that $r_i = s_i^{max} - s_i^{min}$ should be high[1]. Since we know also that $v_i = \frac{p_0 - s_i^{min}}{r_i}$, then v_i should be low in that case if p_0 is a near pixel. $\bar{w}_2$ being the complementary of v_i in the interval $[0, 1]$, it follows that $\bar{w}_2$ should be high. Also $\bar{w}_2$ concords with the transmission and we know that the transmission is inversely proportional to the depth map. The first transmission $\bar{w}_1 = 1$ takes already into consideration near objects as we said previously. From this point, we can see that with this configuration that near objects are well taken into account by the STRESS framework for the dehazing task. (We can also used the Corollary 3.2.1.1 to prove the Proposition: the pixel intensity of near object are roughly very low. The DCP is also another argument.) □

Intuitively for each pixel, the amount of haze we are going to remove, will be relative to $\bar{w}_1$ and $\bar{w}_2$ parameters. So this amount will be low since $\bar{w}_1$ and $\bar{w}_2$ are high. Because we can have a variation of the haze density according to the depth, the near objects will look well dehaze and the far objects will continue to have some haze. If there is no significant variation, the haze should be well removed from the scene as we see with homogeneous haze example. Clearly what we show here is that the radius parameter $R = \max(w, h)$ plays a determinant role on the removing of haze on near objects due to the fact that almost[2] all pixels except

[1] It is not always the case, but often the case.

[2] the width and the height are less than the diagonal

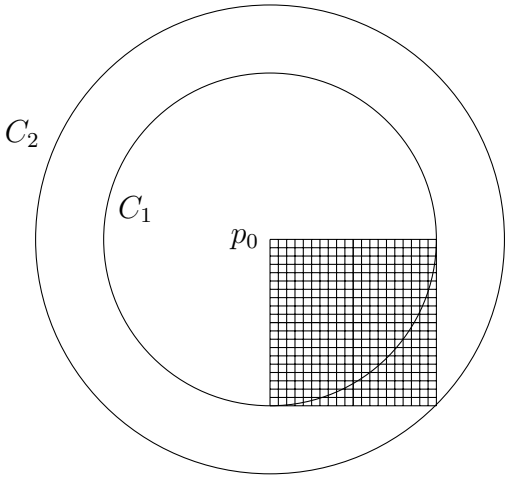

Figure 3.6: C_1 and C_2 are two circles respectively with $R = \sqrt{w^2 + h^2}$ and $R = \max(w, h)$ centered at p_0, the left top pixel

p_0 are candidate for the sampling. We can guess at this point that by somehow reducing or by increasing the R parameter in some way, it will be possible to remove fog from distant objects in the scene. In the next Section we will present how STRESS can be designed on heterogeneous haze - or distance-based haze. Before coming to this point, let's demonstrate the following proposition.

Proposition 3.2.3. *The optimal setting of R, which allows to take into account near objects is such that* $R = \sqrt{image_{width}^2 + image_{height}^2} = \sqrt{w^2 + h^2}$.

Proof. Let's consider the following grill (see Figure 3.6) as a possible shape[1] of our image.

Let p_0 be the left top pixel, C_1 represents a circle of radius, $R_1 = \max(w, h)$ and C_2 a circle of radius, $R_2 = \sqrt{w^2 + h^2}$. With the configuration $R = R_2$, all the pixel of the image except p_0[2] are candidate for the sampling step in STRESS algorithm. Taking $R > R_2$ will not increase the number of samples candidate and also taking $R < R_2$ will not necessarily consider all the pixel except p_0, since R_2 represents the diagonal of the image rectangle or of the image square.

So now let's assume that $R = R_2$. It is also obvious that more we consider pixel for the sampling, more the difference $r_i = s_i^{max} - s_i^{min}$ will be large. And that means, we are making an accurate approximation of the global airlight. And since, we are considering near objects, p_0 and $v_i = \frac{p_0 - s_i^{min}}{r_i}$ will be low. It follows that $\bar{w_2}$ should be high since $\bar{w_2}$ is the complementary of $\bar{v}$ on $[0, 1]$, and the near object well dehazed.

[1] rectangle or square in any case
[2] The pixel in processing

□

In the same manner, if we consider pixel with high intensity[1], we can have two cases since p_0 is such that $E^{min} \leq p_0 \leq E^{max}$. The case $\bar{v}$ is low, and the case $\bar{v}$ is high. For the first case $\bar{w_2}$ is high, the distant objects are not well dehazed and the case $\bar{w_2}$ is low and then they are well dehazed.

From Proposition 3.2.3, increasing the radius more than $R = \sqrt{w^2 + h^2}$ will not going to improve what we already get for near or far objects, so now what about reducing the radius.

It is worth noticing here that the distant objects pixel intensity distribution is different from the sky intensity pixel distribution by considering the DCP when the haze is not dense. In the following, we call small radius, a radius such that $\frac{1}{10}\max(w,h) \leq R = r \leq \frac{1}{2}\max(w,h)$. The radius should be large enough, to include at least the immediate neighbors of a given pixel as candidate for the sampling step.

Empirically, the visual result that we got by setting the radius parameter of the STRESS algorithm at $R = \sqrt{w^2 + h^2}$ is not different from the one with $R = \max(w,h)$.

3.2.3 Heterogeneous non-Dense Haze

For non homogeneous haze, we notice that non-sky far objects are not accurately taken into consideration by the STRESS framework for the configuration where $R = \sqrt{w^2 + h^2}$ or $R = \max(w,h)$.

At first sight, we can guess that by taking a small radius, it is possible to well approximate the removing of fog on distant objects. One hypothesis here is that the haze is not dense and we will make an experiment on a heterogeneous - - one to see whether or not, this setting could influence the distant objects.

Empirically we also observe that for non-sky distant objects, the pixel is also high with some variations due to the Dark Channel Prior. When there is no sky it is also quite difficult to make a difference between a non-sky distant object and a sky region for the pixel situated on the top of the image. Later on, we will come back to this particular observation.

Proposition 3.2.4. *Reducing the radius $R = r$ will allow to remove fog from distant object in non-dense heterogeneous haze.*

Proof. Let consider Figure 3.7 for the proof.

If we take the radius r small instead of taking $R = \max(w,h)$, we can see that the distant object of the scene will be well processed. In fact the difference $r_i = s_i^{max} - s_i^{min}$ is not going to be very large and will roughly be less than $\frac{1}{2}$[2]

[1] distant objects or the sky region

[2] The pixel are normalized on $[0,1]$

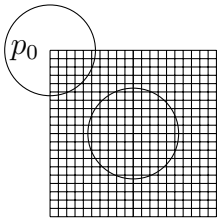

Figure 3.7: the two circles have a radius r chosen such that $\frac{R}{2} \leq r \leq \frac{R}{10}$ where $R = \sqrt{w^2 + h^2}$ or $R = \max(w, h)$.

since we are considering a small spray and far objects[1]. Also, locally the airlight will be well approximated. The non-density of haze will allow us to satisfy the validity of the Dark Channel Prior in some way[2].

Since r_i is not large, At least the term $\frac{1}{r_i}$ in the product $(p_0 - s_i^{min}) * \frac{1}{r_i}$, will be high and making v_i a bit high. If also $p_0 - s_i^{min}$ is large then v_i is also high. It follows that $\bar{w_2}$ is low and the haze on distant object is well removed. (We can also used the Corollary 3.2.1.1: since the radius is reduced, all p_0 close to E^{min} are good candidate for the dehazing process.) □

Empirically, we notice also that near objects are not really taken into account by small radius, but far objects have a good processing for this configuration. Typically, for near objects, we can easily see that the configuration in which we reduce the radius such that $R \leq \frac{1}{2}\max(w, h)$ is not going to improve the visibility of these objects in agreement with what we show in Proposition 3.2.2 and 3.2.3. So depending on how the radius is set, we will work either on globality or locality of the contrast enhancement. Now the idea is to combine different radius in such way that allows to dehaze far and near objects. Subsequently, we will show how this combination can be done theoretically.

3.3 The Theoretical model of haze removing with STRESS framework

According to what we learnt from the previous Chapter and the current Chapter, we can already start to think about the theoretical model that we are going to use to solve the problem. The general idea is of using of a multiscale STRESS framework by combining with insight from state of the art dehazing papers. In the next Section, we will present the multiscale STRESS framework that we will

[1] A far object has a pixel intensity often high and by considering the dark channel for these regions, the difference for neigborhood pixel is not huge.

[2] The DCP is not directly applied to the output image here but we can easily see that the DCP prior is not anymore valid when the haze is dense. The saturation that we get with dense, by using [He et al., 2009] is an empirical validation already. The other point is that the saturation effect tend to be more stronger with small patch (small spray in our case for sky region).

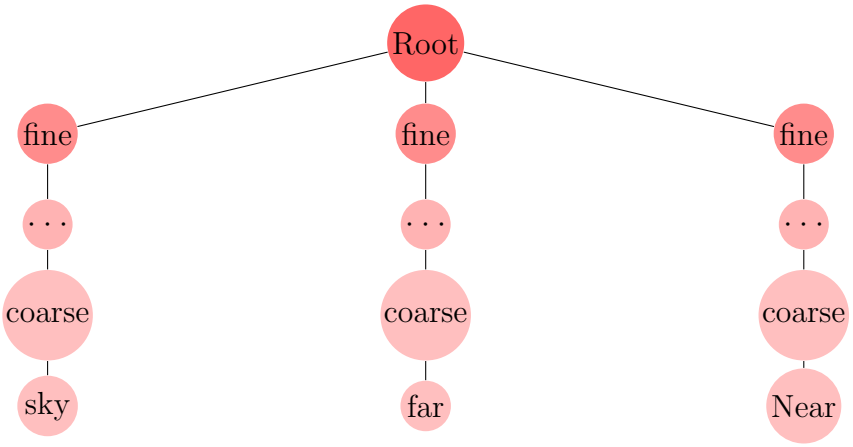

Figure 3.8: General overview of how we model the outdoor hazy image. The root represents the hazy image. We begin at a given leaf and back up to the root. The nodes between a leaf and the root represent an attribute(s) which will allow to refine and determine the real nature of the leaf namely: the sky (or region with the same behaviour like snow region), far objects and near objects. On the last node before the root, we apply a given scale according to the nature of the leaf. An implementation of this tree is showed in Figure 3.11. coarse and fine stand respectively for coarse-scale and fine-scale

be combined with Hidden Markov Model for the defogging task. The second will show a simplified version of the theory developed in Section 3.3.1

3.3.1 The multiscale STRESS combined with HMM idea for dehazing

The key idea behind our approach here is inspired from Fieguth [2011], where it is said concerning HMM that, many complex images, scenes and phenomena can be modelled as combinations of simple pieces. The other papers which also justify our method are the work of Chou et al. [1989] and Graffigne et al. [1995] for instance, where authors show that it is possible to estimate a random field with a multiscale approach. Even their approach is different from what we are presenting here, there is some significant similitude. Our work can be compared to the works of Kratz and Nishino [2009] and Nishino et al. [2012] as well. Our work uses other ideas from the literature of course. The image will be modelised as a graph, where each node will represent a given state or attribute.

From what we develop above, we can see that STRESS is solving already the homogeneous (i.e uniform or stationary) haze case (dense or not). The homogeneous case can be viewed as a single Markov field since we assume there is a single uniform layer that we have to find out. Now what about the heterogeneous case. For the heterogeneous haze, we will also have two cases: one is dense and the other non-dense. Here we will focus mainly on developing a model for non-

dense haze. In fact for the dense case, it is not possible to get more visibility with far objects, simply because the data is not present and for that particular heterogeneous case, the result given by the single scale STRESS is already, one of a pleasing one. Also for that particular case, the dense part will be considered as a sky region and we will process it in the same way that we process the sky. This point will be trivial afterward. Depending on how dense the haze is, we will maybe need to increase the number of samples of STRESS framework parameter, in order to remove noise. The other question according to this point is: How are we going to guess the number of samples needed to remove the noise of a given dense haze. The answer of this question will depend on the way we choose for implementing our case. In our case, we will consider just few samples (less than 6).

We can now imagine a model where we can see the heterogeneous non-dense haze as a superposition of homogeneous haze layer with different density (without being abrupt). It is worth noticing that both the visible pattern and the hidden pattern actually represent two different layers; the goal being to remove these hazy layers to get the dehazed hidden layers. The challenge will then be to guess which radius value corresponds well to the removing of a haze for a given pixel. We can for instance define a cost function which can allow us to choose the best approximation among a finite set of possible approximations. Let us assume that the coarsest scale is given by $R = \max(w, h)$ or $R = \sqrt{w^2 + h^2}$ and the finest one by $r = \frac{1}{10}\max(w, h)$. Let $\hat{p_{0_R}}$ be the approximation of p_0 given by R and $\hat{p_{0_r}}$ be the approximation of p_0 given by r, so we can write:

$$\hat{p_{0_R}} = p_{STRESS,R}\bar{w_{1_R}} + (1 - \bar{w_{2_R}})\bar{r_R} \tag{3.22}$$
$$... = ... \tag{3.23}$$
$$\hat{p_{0_r}} = p_{STRESS,r}\bar{w_{1_r}} + (1 - \bar{w_{2_r}})\bar{r_r} \tag{3.24}$$

From Equation 3.2, the optimisation problem match with the following relationship:

$$|J - p_{STRESS}| < \sigma \Rightarrow |p_0 - \hat{p_0}| < \epsilon \tag{3.25}$$

p_{STRESS} represents a given scale s of the STRESS framework and $\hat{p_0}$ corresponds to the approximation of p_0 at the same scale s. Since we are dealing with a multi-scale approach, the parameter J we are looking for can be obtained as follows:

$$J = \text{argmax}(p_{STRESS,R}, ..., p_{STRESS,r}) \tag{3.26}$$

The problem we want to solve here is a non-stationary problem. The idea is

to carry out some piecewise cut of the image in a such a way that each piece could represent a stationary problem. In other word, we are going to solve the problem by combining STRESS with Hidden Markov Model (HMM) and solve the dehazing issue. Formally speaking, the idea consists of using the Baye's rule in order to check the probability of our hypothesis according to the observed samples and by stating the following equation:

$$p(H|O) = \frac{p(O|H) \cdot p(H)}{p(O)} \tag{3.27}$$

where
H stands for the hypothesis (the final dehazed layer) and O for the observation (the hazy input image).
$p(H|O)$ is called the posterior probability or the probability of H given O, that is the probability of having H after observing O.
$p(O|H)$ is the likelihood and represents the probability of observing O given H.
$p(H)$ is the prior probability or simply the prior and represents the probability of the hypothesis H before O is observed.
$p(O)$ is the marginal likelihood. This factor is the same for all possible hypothesis and can be considered necessary only for normalization purposes. So the Equation 3.27 can be also written:

$$p(H|O) = p(O|H) \cdot p(H) \tag{3.28}$$

Let's assume l being a set of hidden haze-free layers, l_i a given haze-free layer (corresponding to a visible layer) in the image and let's say here that the number of layers in the foggy image is N such that $1 \leq i \leq N$ and $N \geq 1$. For the problem, we are discussing here, if we call I the observed foggy image then we can express the posterior probability as the following:

$$p(l_1, ..., l_N|I) \propto p(I|l_1,)...p(I|l_N) \cdot p([l_1 \cdots l_N]) \tag{3.29}$$

or we can also write the following equivalent form:

$$p(\underline{l}|I) \propto \prod_{1 \leq i \leq N} p(I|l_i)p(\underline{l}) \tag{3.30}$$

where $\underline{l} = [l_1, ..., l_N]$ is a vector. In the literature to solve the Equation 3.30, since we have a multiplicative factor, it is better to use the logarithm function.

In that case the Equation can be written down as follows:

$$-log(p(l_1, ..., l_N|I)) \propto -log(\prod_{1 \leq i \leq N} p(I|l_i)p(\underline{l})) \tag{3.31}$$

If we adopt the same notation as in Hanson [1993] by seperating respectively in the likelihood term and the prior term, we can then write the above relation as the following:

$$-log(p(l|I)) \quad = \quad \Lambda(l) + \Pi(l) \tag{3.32}$$

The goal of this approach being to choose the posteriori, which one represents well what we are looking for (get a good dehazed version of the hazy image). That is:

$$\hat{l} \quad \propto \quad \text{argmax} \quad p(l_1, ..., l_N|I) \tag{3.33}$$

$$\propto \quad \text{argmax} \quad p_{multi\_scale\_STRESS} \tag{3.34}$$

$\hat{l}$ is called the maximum of the posterior probability density function a.k.a the Maximum A Posteriori (MAP) and stands for the best non-foggy layer we are looking for. As for the way we are designing our model, it is possible to see $\hat{l}$ as one of the best layer corresponding to a given visible layer (i.e $\hat{l_i}$ more specifically) or as the best final layer of the entire image resulting from the combination of each best layer. So here we will take the last description as how we will consider the formula 3.33. To solve the Equation 3.33, since we have an ill-posed problem, in the literature, we have often go to use some optimization algorithms like graph-cut or to use a Laplacian regularization. In our case, the good news is that with STRESS we can already find a good approximation of the layers, we are looking for as we show above in the previous development: For near objects[1], the radius is R and for far objects the radius is r.

So now the problem can be summarized as the following: For a given pixel in the input which single scale STRESS represents the best layer for the dehazing task.It is worth noticing here the fact that l is the combination or not of many other layers representing the STRESS framework at variing scale.

The multiscale approach is a challenging one to implement since we assume that we can have 1, 2, $\cdots$, N different state variables. Also from what we did so far, we know for instance that STRESS process well the near objects for default setting of the radius, but do not really, as far as objects are concerned. The idea is to assume that we have found the hidden layer of near objects and how we are

[1]near objects, sky region and regions which have the same behaviour with the sky like large snow area. We will notice this in the following lines.

going to find the hidden layer of far objects. We will be discussing this question in the next Section by assuming that we are looking for just two patterns in order to dehaze the hazy images.

3.3.2 The two-scale-STRESS combined with HMM idea for dehazing

Without taking into account, what we noticed empirically, we should assume a multiscale model instead of trying to solve the problem with two-scale-approach. But at the same time if we take into consideration what we get from these first observations, the STRESS algorithm is solving the dehazing task already for near objects. So our intuition is to suppose that, while solving the problem with far objects. It is worth noticing that with STRESS, we can have a solution for the problem for a given pixel. Here we have $N = 2$. The other reason why we do not adopt at this point more than two-scale is the cost.

Since the output pixel of the two-scale-STRESS is a potential solution of our problem, how are we going to remember which one is the best? The formulation of the DCP will help us to do it in some way. In this work we do not use the DCP directly but our procedure seems to be near to that idea. It is also good to remember that STRESS does not consider patches in the rectangular way but in the circular fashion. So the theoretical transition probability corresponding to the coarsest prior to the finest one - the coarse-to-fine transition probabilities [Perez, 1998] - is as the following:

$$p(l_{k+1}|l_k...l_0) \quad = \quad p(l_{k+1}|l_k) \tag{3.35}$$

Where $(k+1) \in \{0,1\}$ and $k \in \{0,1\}$[1] since we are considering just two-scale. So from the definition of the prior in Equation 3.35 the J parameter we are hunting can be assessed when the following formula holds for near and far objects:

$$\text{argmax}(|p_0 - \hat{p_{0_R}}|, |p_0 - \hat{p_{0_r}}|) \sim \min\left(p_{STRESS,R}, p_{STRESS,r}\right) \tag{3.36}$$

Our idea for applying this transition is of course by choosing the minimum pixel value (the dark channel) for each channel between the results given by the two-scale. One drawback by choosing the dark channel and just two-scale (instead of multiscale) can be the smoothness issue of the final output and also the scales can be mixed[2]. In other hand, the advantage of our modelling is simplicity.

[1] Equivalently, we can write $(k+1) \equiv 0 \mod 2$ or $(k+1) \equiv 1 \mod 2$ and $k \equiv 0 \mod 2$ or $k \equiv 1 \mod 2$.

[2] Theoretically, for far objects, we know that the output pixel intensity with the radius r should be lower than the output pixel intensity value with the radius R and we have the inverse scenario with near objects. However even if in practice, the previous assertions are true for a majority of cases, it may so happen that, they are false for some pixels. And for those cases, by choosing the minimum pixel intensity value, the scales output are going to be mixed since we have 3 channels (total order vs. partial order problem). A typical example of the complexity of

Algorithm 1 Two-scale-STRESS for dehazing

Require: $R_1 = R = \max(w,h)$ or $R_1 = R = \sqrt{w^2+h^2}$ and $R_2 = r = \frac{1}{10}\max(w,h)$ or $R_2 = r = \frac{1}{10}\sqrt{w^2+h^2}$
Ensure: $\bar{w_2}_1 \approx 1$ and $\bar{w_2}_2 \approx 0$
1: **Foreach:** $c \in C$ **do**
2: **Foreach:** $p_0 \in c$ **do**
3: Compute p_{STRESS,c,R_1} such that
4:

$$p_{STRESS,c,R_1} = STRESS(p_0, R_1, n_i, n_s) \tag{3.37}$$

5: Compute p_{STRESS,c,R_2} such that
6:

$$p_{STRESS,c,R_2} = STRESS(p_0, R_2, n_i, n_s) \tag{3.38}$$

7: **end for**
8: **return** $p_{Two\_Scale\_STRESS,c} = \text{argmax}\ (p_{STRESS,c,R_1}, p_{STRESS,c,R_2})$
9: **end for**

In the Algorithm 1, we assume that we have a RGB image represented by 8-bit per channel, a channel is named c and the set of the 3 channels by C, R_1 represents the first scale and R_2 the second scale of the STRESS framework. Even here, if we consider 3 channels, it is also possible to work on a grayscale image. For this kind of set-up, especially for R_2 we assume that the image width and height of the input is at least 200, since we do not want the radius to be too small. $\bar{w_2}_1$ represents the transmission related to R_1 and $\bar{w_2}_2$, the one related to R_2. $STRESS(p_0, R_1, n_i, n_s)$ and $STRESS(p_0, R_2, n_i, n_s)$ the STRESS algorithm with different radius, but other parameters are the same.

After the computation of the two-scale-STRESS, we compute and return on line 8 the most dark pixel by assuming as a prior that in the haze-free image, the pixel should be more dark than in the hazy image. We will call this prior the Generalized Dark Channel Prior (GDCP) to underline the fact that all the channels are dark.

The way the prior is chosen, is just trivial, even if deducting it from the DCP, we can already anticipate the fact that this solution may not be the best one (at least one channel is dark for a given pixel, not systematically all the 3 channels). The pre-condition for this algorithm is a heterogeneous hazy non-dense image. So how can it be sure that this pre-condition is satisfied? We will see soon that the homogeneity criteria is hard to assess since in real life, the haze density is changing with the depth information. As a general rule, though, if we assume

this kind of issue is shown in [Deborah et al., 2015].

that the haze is homogeneous, then we can assess the density criterion in some way. We will come to this point later.

(a1) (b1) (c1)

Figure 3.9: (a1) The original hazy image, (b1) STRESS, (c1) The two-scale STRESS. Here the sky does not have a large area and this area is mixed with dark objects (tree branches or trunks)

(a2) (b2) (c2)

Figure 3.10: (a2) The original hazy image, (b2) STRESS, (c2) The two-scale STRESS. It seems here that taken the envelope minimum from the two-scale is not a good strategy for the sky region.

Here are some results that we get from the Algorithm 1. From this, we have some trouble with the sky region and that makes sense because the GDCP could not be valid in the sky, even for blue-sky, we observed that the DCP can be valid. By taking a kind of contrapositive of the DCP, we will have the following statement.

Remark. *All color channel in haze-free image has pixel with high intensity and close to* 255*, if we consider an image with* 8 *bit per channel for sky region*

With the prior representing in the remark above, we will develop in upcoming sections a new model for haze removal which will combine HMM with edge detection and the two-scale-STRESS.

3.3.3 HMM idea combined with Edge Detection and two-scale-STRESS for the Dehazing task

First of all, from the previous experiments, it is worth noticing that the saturation effect that we get in the sky region comes from the fact that we have two radius and we are using the GDCP as a prior to take into account the far objects. Unfortunately, by using the GDCP approach for the two-scale, we do not get a visually pleasing image for the sky region.

The good news about how to solve this issue is that setting the radius at $R = \sqrt{w^2 + h^2}$ or $R = \max(w, h)$, helps us to remove homogeneous part of the haze typically from near objects, far objects and sky region when the haze is heterogeneous and dense, without getting saturation effect in the sky. Also experimentally, when we compare the result of the two-scale-STRESS in the previous section, we notice that they can be viewed as two envelopes. One representing the upper-bound envelope $E^{max}_{two\_scale\_STRESS}$ and the second one the lower-bound envelope $E^{min}_{two\_scale\_STRESS}$. In the sky, by choosing the envelope $E^{min}_{two\_scale\_STRESS}$ we do not take the best approximation of the sky. And that makes sense, since we know from the STRESS framework, the output of STRESS should be near to the envelope E^{max} when the pixel value is high as the one in sky. So there is a direct connection or a correlation between E^{max} and $E^{max}_{two\_scale\_STRESS}$ versus E^{min} and $E^{min}_{two\_scale\_STRESS}$ since we know about [He et al., 2009] prior and the Remark 3.3.2. These last observations can already give us an idea of a simple function which could allow us to take decision for the multiscale STRESS dehazing algorithm presented above.

So if we can decompose the image in almost three regions (sky, far and near objects[1]), we can then apply different scale for each region and get the dehazed output with less saturation. Here again, the idea is to use the idea of Hidden Markov Model in each sub-regions. So now the question with this new approach is how are we going to distinguish them.

There is a lot of approaches in the literature, which can help us to find the 3 regions for instance edge detection, graph-cut, gibbs model, annealing, Local Binary Pattern (LBP), etc. Also in the literature it is possible to find some interesting approaches using machine learning tools or pattern recognition as in [Gallagher et al., 2004], but often these methods are not accurate. In our case, due to simplicity purposes, and because the current analysis is just a part of our first implementation, we want a sparse representation. This sparse representation can allow us to take a quick decision[2] about the processing of a given pixel in

[1] We will see later on that a potential region which has a high intensity value (snow for instance) could be critical, as the way we are processing. At the same time, if we can find out these three regions in an image, that means that our model is valid for near objects and sky region. Objects in the scene which have far label, we need sometimes to check their pixel intensities for some scenarios.

[2] We also want a fast prototyping to quickly check out our hypothesis.

the hazy image. So the final method that we choose among the ones we present earlier is the edge detection, but other segmentation methods can be applied[1].

The main idea behind the edge detection strategy (for this first iteration) is that we notice in most cases in hazy images and their corresponding free-haze images, the sky a priori does not contain any edge since we do not have cloud often in hazy images. And even if it is possible to find clouds on a hazy image, they are very rare and their proportions are not significant.

The second reason is that, the sky is on the top region in the image, which means that the first edge which can be found will belong to far objects in the case of a non-homogeneous haze and to near objects in the case of a homogeneous haze.

The third reason why we choose the edge detection at this stage can be assigned to the fact that image in which we do not have the sky, we do have a high intensity value for the pixel which is in the top lines of the image. In that case if we just consider a labelling with high pixel intensity value for segmentation, we can easily make a false detection - false positives - of the sky region. We are not saying that our strategy is unquestionable but we will show later in the experiment part that this approach is robust at least for all images that we tested from state-of-the-art dehazing papers.

Now let explain more the edge detection choice. Before developing different method we tried here, it is worth noticing that the sky region detection can be either think as a preprocessing step or postprocessing step. In the Subsection 3.3.3.4, we will define the trip concept. Basically a trip can be viewed as finding the first edge in the column vector of an image matrix. So we will define two simple solutions for the preprocessing step. One is very simple and is not really costly and not robust, the other is more robust and time consuming. The second solution can be also viewed as the complementary of the first solution, in the case it is really hard to take a decision about the presence or the absence of the sky.

3.3.3.1 First preprocessing solution

For the edge detection algorithm, we will use Canny edge detector [Canny, 1986] with a multiscale approach on a hazy input images. Two thresholds t_1 and t_2 will be used separately to detect the presence or the absence of the sky region. t_1 and t_2 are such that $t_1 < t_2$ and t_1 is enough strong to remove false detection in most of case. We found that $t_1 = 10$ is already strong enough to generally permit to avoid false detection. t_2 is the threshold that we will use to detect how dense is a given input hazy image. We will explain this point later. Here we can have roughly three cases:

1. If the processing with the Canny edge detector with the parameter t_1 allows

[1] We will see later on, if this approach is robust or not in the experiment part.

us to detect very soon the presence of edges for the majority[1] of trips, then we take directly the decision, that the input does not contain sky and apply immediately the Algorithm 1.

2. For most of the trips, the first edge is not found very soon so that we can confirm the presence of some data. In that case we apply the second scale to see if the sky-region found is reliable. This reliability will be on the proportion of finding the first edge on all the trips. We do not consider anymore the sky region pixel value when the proportion between the two scales is huge. Since this point, we can see already that it might happen, that our voting algorithm fails. We will show in the next chapter that it possible to detect this failure.
3. The third scenario is that our voting algorithm is not able to say if there is a sky or not. We do not have this case in our database in fact, but if that happens, we do not consider the region as a sky region.

3.3.3.2 Second preprocessing solution

The trip concept is not all the time true. We can for instance have an important area of sky region in an image and not be able to detect it with the trip concept[2] since we are assuming that the sky is on the top of the image. So a more robust design is likely to explicitly label our input image according to two attributes: the presence/absence of edge for a given pixel and its intensity value. We do not implement this here[3]. The key idea is to check twice the presence or the absence of the sky region on the image. The first verification corresponds to the first and second point of what we describe in Subsection 3.3.3.1 and the second verification based on the labelling process that we describe here.

In the next Subsection, we will give an overview of the framework for both dense, non dense (homogeneous/heterogeneous) haze.

3.3.3.3 The general framework for dehazing

In real life, a homogeneous haze is extremely rare. The haze being mixed with the data, it is hard to assess the homogeneity criterion for non-dense haze. However the density criterion can be assessed in some way. This knowledge will help us for defining the parameter corresponding to the number of samples in order to remove noise when the haze is dense and homogeneous[4]. In the following, we assume as precondition that there is a homogeneous fog in the input image. In that case, if the haze is dense then, the percentage of edge should be low and also by considering two edges maps with different parameters t_1 and t_2, the proportion

[1] Our voting algorithm will be presented later.

[2] If we have an image with a lot of noise, noise in the sky can become edges when using Canny edge detector.

[3] The entire image is not labelled.

[4] Finally even if we implement this, we do not take into account of that because we fixed the number of samples $n_s = 5$ for our method.

of edges between these two-scale will vary significantly if we assume that the haze is homogeneous and even if the interval between t_1 and t_2 is not big. Here we set $t_1 = 10$ and $t_2 = 15$. If the haze is dense but not homogeneous, the haze in dense part, will be considered as a sky region since the data of this region is not available. The density criterion will be valid when we assume implicitly that the haze is homogeneous. If the haze is non-dense, the number of edges should be high at t_1. Even if our assumption about the density of haze is not really strong, this assumption works on the majority of images that we test.

One key concept in the Algorithm 2 is the introduction of the trip concept which allows us to decide whether or not we have a significant sky area which should be taken into account.

Algorithm 2 Voting algorithm for detecting the presence of a significant sky area

Require: Hazy images
Ensure: Labelise the input image as dense or non-dense haze
1: Compute the edge map $Edge\_Map_1$ corresponding to t_1
2: Compute the edge map $Edge\_Map_2$ corresponding to t_2
3: Compute for each map, the average of finding the first edge for all the trips
4: Decide the presence or the absence of the sky according to these percentages

In the algorithm 2, on line 4, the decision is based on the fact we do not have edge on the top of the image, the pixel intensity is also greater than 60. Futhermore the area which has these two attributes ("no edge" and $intensity > 60$) should represents at least 5% of the total height of the image and 50% of the total width.

In the Algorithm 3, the step for determining the haze density is now optional since we fix the number of samples less than 6.

There is a simple way to decide whether or not the potential sky region should be taken into account. This simple way is based on three attributes: the consecutivity of potential sky area, the depth of this area and the pixel colour intensity. For this first iteration of our implementation, the consecutivity will not be going to take into account, for simplicity. Here also, we use the trip concept with its limitations. In Section B.3 of Appendix B, we will present the data that we get from each intermediate step which help us to take a decision. That will give us some ideas of how to improve the general framework in future.

Our final framework can be summarized as a simplified Expectation-Maximization (EM) algorithm as the one described in [Fieguth, 2011] as the following:

Algorithm 3 General Framework overview

Require: Hazy images
Ensure: Dehaze the input image
1: Decision about the presence or the absence of the sky region
{Comment: Depending on two attributes corresponding on the two-scale t_1 and t_2 of the Canny edges detector algorithm}
2: (Optional) Decision about the density of the haze, depending on two parameters:

- the number of edges from the first scale t_1
- the number of edges from the second scale t_2

Compute the variation between these two parameters and decide whether or not, the haze is dense.
3: The decision about the lower bound of the bright pixel is taken
4: Apply then the two-scale-STRESS algorithm

Algorithm 4 Simplified Expectation Maximization

Require: Hazy images
Ensure: Estimate the hidden layer $\hat{\theta}$ for hidden field U
1: Initialize $\hat{\theta}$
2: **while** not converged **do**
3: E-Step: Given model parameter $\hat{\theta}$, compute the hidden estimates $\hat{U} \leftarrow E[U|Z, \hat{\theta}]$
4: M-Step: Given hidden estimates $\hat{U}$, Compute ML estimate $\hat{\theta} \leftarrow \operatorname{argmax} p(U|\theta)$
5: **end while**

In the Algorithm 4, the expectation step (E-Step) is doing with the two-scale computation and the maximization step (M-Step) by finding the best state correspesding to information from the E-Step[1] and the potential sky region.

3.3.3.4 Implementation issue

For this part, it worth noticing that our approach will consist of the iteration of a given current implementation in order to correct a given failure case. Here we will present at least the first and the second iteration. We present in Figure 3.11, the implementation corresponding to the first iteration.

Let consider the following 10 by 3 matrix as edge map obtained from a 10 by

[1] roughly depend on attributes R and r

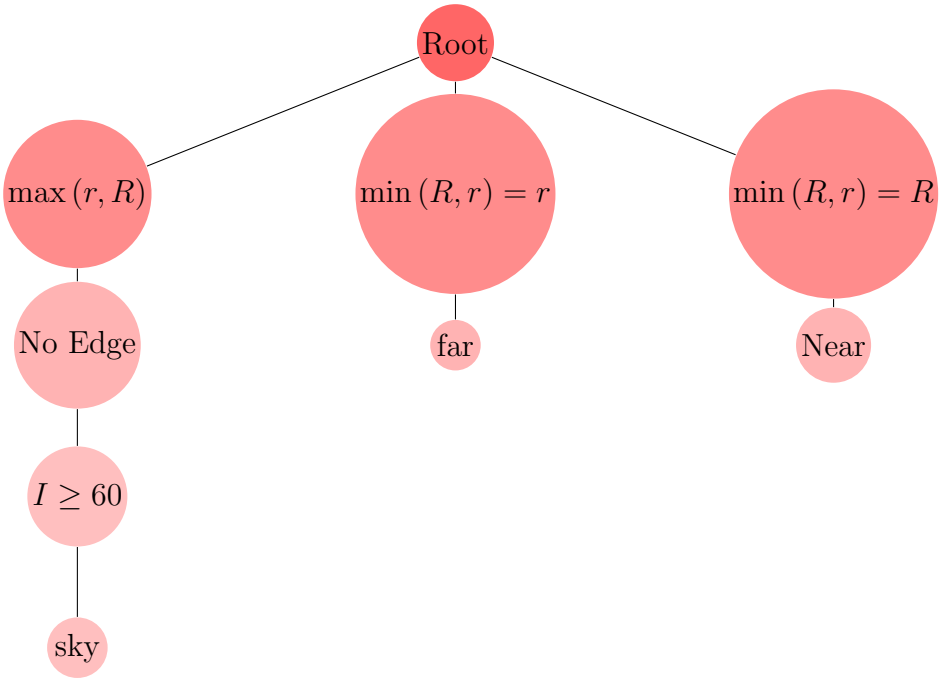

Figure 3.11: An implementation of Figure 3.8. We begin by checking the presence or the abscence of the sky region, followed by far or near objects. On the right branch, we also check at the node "No edge" the width and the height of the region.

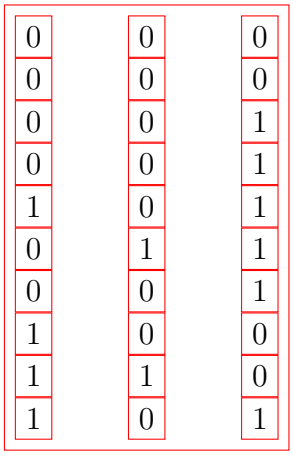

Figure 3.12: Vertically we have: $\frac{40+50+20}{3} \approx 36\%$. Horizontally:
1^{st} trip: No edge $> 5\%$ (Yes), 2^{nd} trip: No edge $> 5\%$ (Yes), 3^{rd} trip: No edge $> 5\%$ (Yes), So we have the majority of trip which do not have edge with pixel intensity > 60 which is interpreted as having a sky region there.

3 RGB image. A trip will represent a subset of a given column from the first top zero value to the first 1 (corresponding to the first edge) met in that column.

For this kind of image, we will check if the height and the width of the region which do not contain edge is significant. For the height, we will check, if this region covers the 5% of the total image height and for the width, at least the 50% of the total width of the image. The region also should have high intensity value (At least 60[1] for an image with 8 bit per pixel.).

Here, we can already see that, our approach can have some false detection of the sky region or miss sometimes the sky region. Also if there is a pattern on the image which has the same behaviour with the sky region and is not on the top of the image, this pattern can be missed by our algorithm as we will see for the failure case in the next chapter.

The main difficulty of our work since we know that STRESS can solve the problem is to know which label a given pixel has, in order to apply the STRESS algorithm with the good parameters to that particular pixel. So our problem can be seen as a labelling problem. If we solve efficiently this labelling problem, then theoretically, the problem is solved by STRESS.

One goal here, is to apply the Remark 3.3.2 by looking for the minimum pixel intensity[2] of a potential sky area. The issue by searching this minimum is that sometimes, the first edge found is not exactly the one we are looking for and the

[1] When the sky is blue, we can have some channel with value around 60. Here we allow value greater or equal to 60.

[2] The minimum containing in all trips. Since we are considering the trips, this minimum is by definition high for white sky and maybe a bit low for blue one.

one found is an outlier. We design a voting algorithm[1] which takes into account the occurence or the score of pixels belonging to the potential sky area. The intensity of these pixels should vary between 60 to 255. The count is done by range of 10 elements. So we consider the pixel of same range as equivalent. Typically we have the following ranges $60-69$, $70-79$, ... $250-260$. These outliers being very low, the minimum score considered is 20. So the first range from 60 which has a score more or equal to 20 will be choose as a good candidate. For instance, let's assume that we have the following configuration:

- $score(60-69) = 0$
- $\cdots$
- $score(140-149) = 9$
- $score(150-159) = 21$
- $score(160-159) = 301$
- $score(170-159) = 1021$
- $score(180-159) = 0$
- $score(250-260) = 0$

The range which will be chosen is $150-159$[2]. Then when we are processing, for any pixel which has at least a value higher or equal to 150 in all the 3 channels, we will assign the max of the two-scale-STRESS in the first iteration of the application, and the scale with radius R of the STRESS framework in the second iteration of the application. We will see in the next chapter with an example that the remark 3.3.2 can be critical for pixel with high intensity and which does not belong to the sky region. This issue can be avoid by labelling the image pixel.

The goal of this algorithm is not to detect the sky region formally[3] but to know if there is a sky eventually by using simple priors about outdoor hazy images. The potential sky area should be on the top of the image, and covering a large area. This area has also two other attributes: No edge and color intensity. As we said earlier, if there is a region on the image which behaves as a sky region and we do not find sky, our algorithm can fail. An example of this failure is given in Figure 4.32.

[1] There are many advanced approaches as the one in [Bellet et al., 2014]. Here for reasons we enumate above, we implement a simple approach which allows to check out quickly our hypothesis.

[2] $160-169$ could be a more robust range since the difference of the two ranges is huge - greater than 100. So one can design a more robust algorithm which takes the second best range since the first one is too close to the threshold.

[3] Image understanding or semantic image retrieval

Also to decide whether we are processing near objects or far objects, since the radius is the attribute allowing to approximate these objects, we take just the darkest pixel intensity from the two-scale-STRESS by assuming the GDCP. This allows to avoid a global labelling of the image into (sky, far and near objects) for these first iterations. We will see later on, even if our implementation seems to work well for most of images that we test, we should refine it in the future work in order to have a more robust solution.

4 Experiment, Results and Evaluation

In our experiment set-up, we will consider three types of images. Images taken in Gjøvik, images from NRK and images from state-of-the-art algorithms. Gjøvik pictures and the ones from NRK are initially very large and make the computation time really high. To avoid this, we reduce the original size to 1128×751 for Gjøvik pictures and 1128×635 for NRK pictures. All the codes that we have were run on the following machine: Ubuntu 14.04 LTS, with 8GIB of memory, Intel Xeon (R) CPU E31270 and 3.45GHZ $\times 8$.

For Gjøvik pictures the original images have size of 4290×2856 and format $CR2$ from a camera model Canon $450D$. Then we use dcraw software to convert the initial file into BMP files. From the obtained files, we use next ImageMagick to resize all the image to 1128×751

For NRK pictures, the original frames have size of 1920×1080, we do exactly the same procedure as previously except the fact that we use VLC software to extract images from videos. The retrieved files have finally size of 1128×635. In the following, we call our database, Gjøvik pictures or NRK pictures.

At first, we show the first part of our experiment by presenting 5 different images see figures Fig. 4.13 to 4.20, then the second part for the rest of images which contains the results of state-of-the-art algorithms compared to STRESS and ours based on the STRESS.

Basically, for the first experiment, we have:

- (a): represents the original hazy images from our database.
- (b) Images which have this label are processed by McCann99 algorithm presented in Funt et al. [2000]. $Iter = 4$ represents the parameter number of iterations.
- (c): represents the result given by ACE algorithm, here we take the Getreuer [2012] implementation available from the following website[1]. The implementation is very fast because a parallelism approach is used. All the outputs in this paper use $\alpha = 8$.
- (d) we use the Median Dark Channel prior presented in Gibson et al. [2012] with a window 5×5. We do not take the same size as in (f), because some strange effects appear sometimes in window parameter 15×15. We implement this code using a part of the code of DCP code.

[1] http://dev.ipol.im/

- (e) this group represents the output of the method presented in Tarel and Hautière [2009], here we keep the default parameters of the implementation given by authors. The code is available on internet[1].
- (f) represents the Dark Channel Prior (DCP or DC) developed by He et al. [2009] with a window 15×15. As the authors say in their paper, with a small patch the result looks saturated. We try a coupled of window size and effectively, we notice that. In our experiment, we use also patch 30×30 and 50×50. The code is available on internet[2].
- (g) represent the result by STRESS for different parameters. Here the rule, we try to respect about how we choose these parameters is to have approximately the same number of processing for each single pixel. For instance in the case of $n_i = 150$ and $n_s = 5$ the final processing number is $n_{processing} = 150 * 5 = 750$, so then when we use $n_s = 20$, to have the same processing number for each pixel, we take $n_i = n_{processing}/n_s = 750/20 = 37.5 \approx 38$. $R = \max(image_{width}, image_{height})$. We use for this first part $n_s = 20$ and $n_i = 38$
- (h) stands for the first implementation of our approach. In this paper, since we are using the DGCP, we choose the number of samples low as we said in the previous Chapter ($n_s = 5$) and by following the rule above in (g).

Generally for STRESS, we observe that keeping the number of samples (n_s) lower than 6 and maintaining iterations number (n_i) less or equal to 150 give a relatively good dehazed output with a good contrast and the processing time is also reasonable (less than 2mn30s for an image of size 1128×635 in average). But sometimes by doing this, due to the fact that the original hazy image contains a few relevant information (Figure 4.13 where the only relevant information is the athlete), we observe that the output can be noisy. To avoid this, we decide to use more samples ($ns = 20$) in a way that finally we have the same processing number for each pixel. And the good news is that the cost in time looks very near to the configuration $n_i = 150, n_s = 5$ and even better (we got approximatively 2mn for an image of size 1128×635 in average).

For the second part of experiment, state-of-the-art images results are taken from internet[3]. The original hazy input image is then run with STRESS with one or two different configurations as presented above.

Considering the psychophysical experiment, 3 images of our database from a total of 20 and 4[4] images of the state-of-the-art, from a total of 32, are evaluated

[1] http://perso.lcpc.fr/tarel.jean-philippe/publis/iccv09.html

[2] https://github.com/akutta/Haze-Removal

[3] http://www.cs.huji.ac.il/ raananf/projects/dehaze_cl/results/

[4] Here we have in total 7 images. ISO 204621 reports that the number of test stimuli should be equal to or exceed three scenes, and preferably be equal to or exceed six scenes [ISO 204621:1994]. For colour image, Field indicates that between five and ten images are required to evaluate quality issues.

by 19 participants[1].

In the case of the psychophysical experiment, we use a web-based tool for psychometric image evaluation tool named QuickEval[2]. It is good noting that the experiment is made in uncontrolled environment. According to [Sprow et al., 2009], research have shown small differences between controlled and uncontrolled experiments. The presentation of stimuli is done via a monitor. The area immediately surrounding the displayed image and its borders has a neutral dark grey color. Before commencing the full-scale experiment with the 19 paricipants, we make a tryal experiment with two observers, to test the experimental set-up. From this, it seems that the person who has a direct explanation of the instruction of the experiment finish quickly.

Evaluations of our algorithm take mainly into account the visibility level for both the metric-based and psychophysical one.

The metric-based experiment shows that our algorithms has satisfying results, whereas the psychophysical one demontrates that our results are encouraging when the hazy image is taken from our database and are quite close to results of previous dehazing algorithms when we choose the image from state-of-the-art images.

4.1 Images from our database

Figure 4.13	e	$\bar{\gamma}$	σ
(b)	0.76	1.42	0.003
(c)	87.87	3.92	0.04
(d)	81.51	3.30	1.34
(e)	123.36	7.49	1.66
(f)	82.27	5.15	0.99
(g)	85.66	10.00	1.50
(h)	76.05	21.25	2.12

Table 4.3: Corresponding to Figure 4.13

From Figure 4.13, we can say that the main drawback of our method is the lost of colour fidelity. As it is said in [El Khoury et al., 2014] the dehazing task does not preserve the colour fidelity. Also here the STRESS (g) is set such as $n_i = 38$ and $n_s = 20$ seems to be the best output. Generally, we notice empirically that this kind of setting in which the number of samples is bigger than 10 is not good for the dehazing task. For our output, we have $n_i = 150$ and $n_s = 5$.

[1] [Engeldrum, 2000] recommends between 10 and 30 observers are recommended for typical scaling applications as the one in [Simone et al., 2010].

[2] more information at: http://www.ansatt.hig.no/mariusp/quick/login.php?redirect=index.php

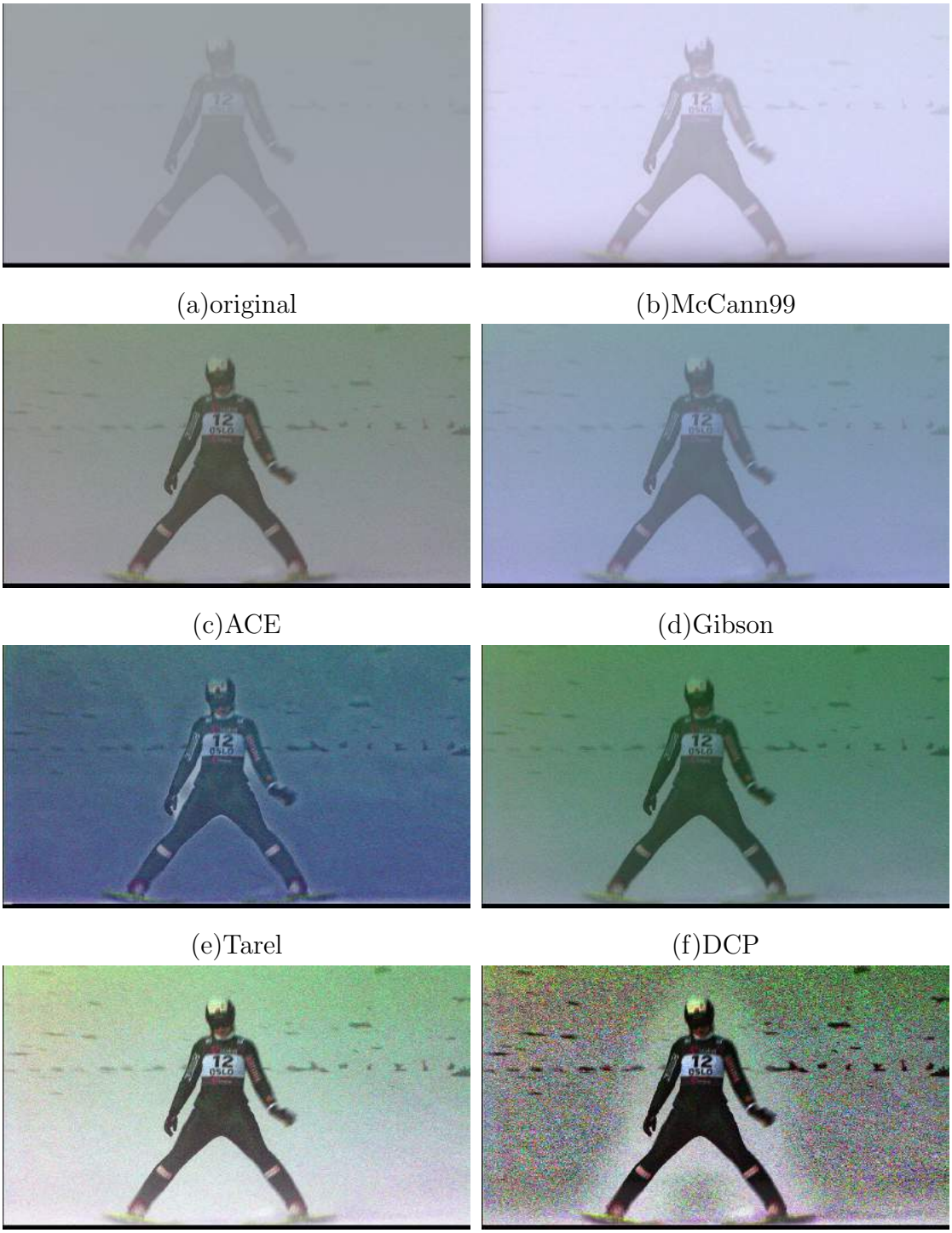

(a)original (b)McCann99

(c)ACE (d)Gibson

(e)Tarel (f)DCP

(g)STRESS (h)ours

Figure 4.13: NRK1. Image courtesy NRK Sport Event

As it is said in [Tarel and Hautière, 2009], and considering Table 4.3, the image which has e, $\bar{\gamma}$ high and σ low is the best for this metric. At the same time, none of these image has this criterion. Here for instance, the parameter e is very high for (d) Tarel and (c) ACE. The parameter $\bar{\gamma}$ is somehow high for our approach based on STRESS and STRESS also. With regard to the third parameter σ, its value is very low with (b) and (c). So it is quiet difficult to say which one of these images is the best one in term of these metrics.

(a) original

(b) McCann99

(c) ACE

(d) Gibson

(e) Tarel

(f) DCP

(g) STRESS

(h) Ours

Figure 4.14: NRK 2. Image courtesy NRK Sport Event.

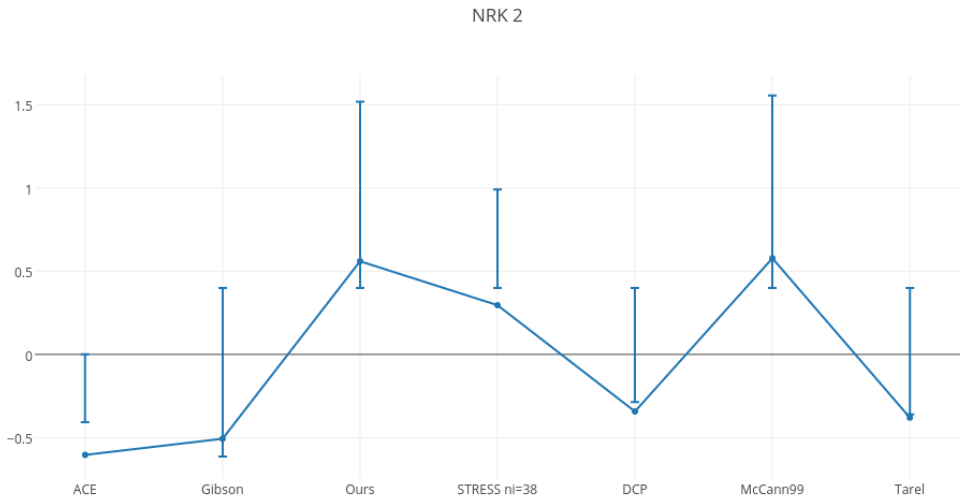

Figure 4.15: Psychophysical results for NRK 2

From Figure 4.14, we can notice the fact that far objects seem to have more visility in our case and the colour of snow does not look saturated for our approach.

In the Table 4.4, unlike the previous case, here the parameter e is one of the highest for our method and $\bar{\gamma}$ is the highest. So considering these two metrics, our method is one the best one. However, we have the worst score considering the third parameter σ, which should be low. For this series, concerning the psychophysical experiment, McCann and ours have the best rank but Tarel method which has one of the best rank for the metric-based evaluation do not get the same grade for the

Figure 4.14	e	$\bar{\gamma}$	σ
(b)	0.28	1.45	0.005
(c)	2.15	2.34	0.04
(d)	2.21	1.65	1.39
(e)	4.06	5.05	1.72
(f)	2.13	1.46	1.62
(g)	2.32	2.81	1.53
(h)	3.14	5.31	1.86

Table 4.4: Corresponding to Figure 4.14

subjestive evaluation. At the same time Tarel method has a positive upper-bound Confidence Interval (CI) unlike Gibson.

(a) Original

(b) McCann99

(c) ACE

(d) Gibson

(e) Tarel

(f) DCP

(g) STRESS

(h) Ours

Figure 4.16: Gjøvik 1. Image taken in Gjøvik in winter 2014-2015.

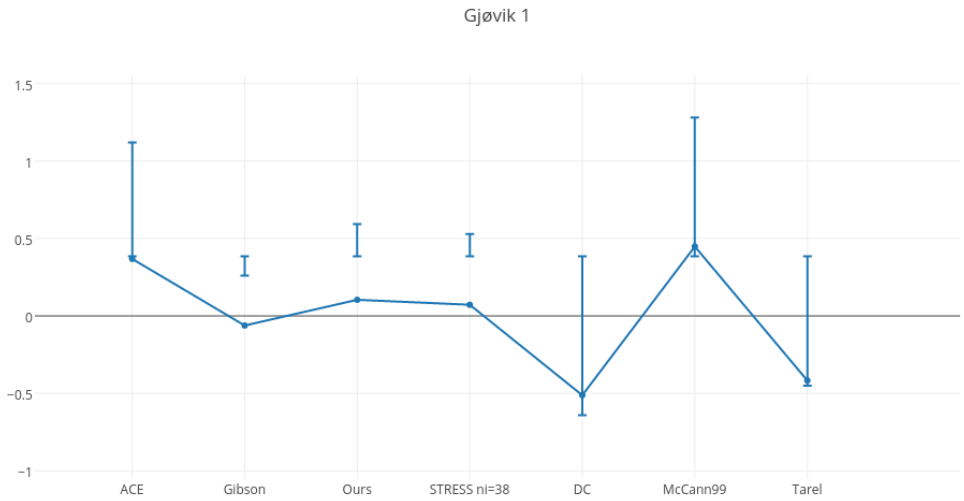

Figure 4.17: Psychophysical experiment for Gjøvik 1

Figure 4.16	e	$\bar{\gamma}$	σ
(b)	-0.06	0.77	$3.93e-05$
(c)	0.07	1.56	0.0002
(d)	0.67	1.59	0.08
(e)	2.27	3.50	0.0
(f)	1.61	2.16	0.18
(g)	0.14	1.36	0.41
(h)	0.49	1.86	1.08

Table 4.5: Corresponding to Figure 4.16

The Figure 4.16 shows that MacCann, Gibson, Tarel and the DCP get saturated but STRESS, ACE and ours don't. Also the far objects are more visible in our case.

The Table 4.5 shows the best approach is the one implemented in (e). And even we have hallow effect and saturation in the sky, it seems that the image in (e) is the one which has more visibility for these metrics. And the question from that could be: Is this metric always reflect well this visibility criterion? The other thing is that for instance McCann approach , we could not say something considering the metric-based experiment because the first two parameter e and $\bar{\gamma}$ are very low - which is not good - but σ has the lowest value - which is good. Now

when considering the psychophysical experiment McCann has the best ranking followed by ACE and our method.

(a) Original

(b) McCann99

(c) ACE

(d) Gibson

(e) Tarel

(f) DCP

(g) STRESS

(h) Ours

Figure 4.18: Gjøvik 2. Image taken in Gjøvik in winter 2014-2015.

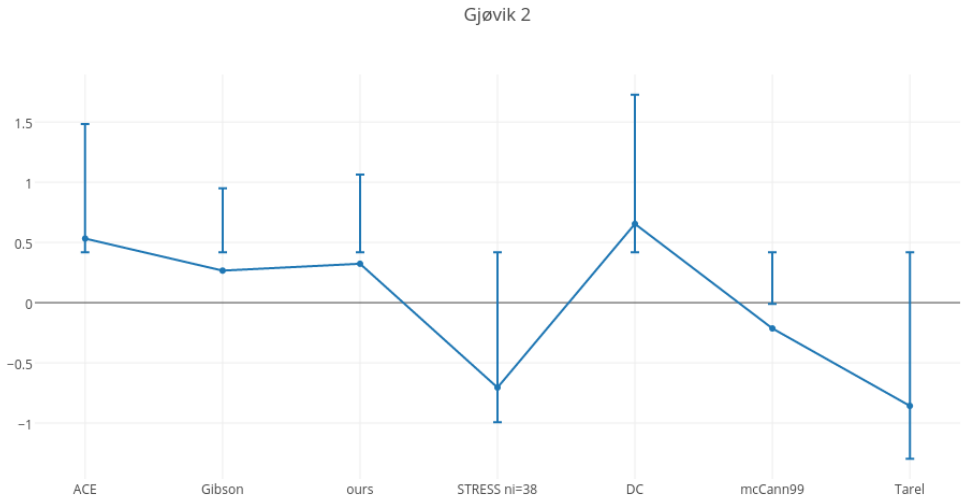

(h) Ours

Figure 4.19: Psychophysical experiment for Gjøvik 2

In Figure 4.18, MacCann, ACE, STRESS and ours have trouble with color fidelity but this effect is less noticed with Gibson, Tarel and DCP.

Our method has the best score according to the parameter $\bar{\gamma}$ since we have the highest value and also the parameter e is the second highest one. Visually we can notice that there is no saturation effect.

The psychometric evaluation ranks our method third behind ACE and DCP, so here we can see more correlation between the two types of evaluation. Tarel

Figure 4.18	e	$\bar{\gamma}$	σ
(b)	0.27	1.36	0
(c)	1.41	$1.96e-04$	2.26
(d)	1.15	0.06	2.36
(e)	2.50	2.98	0
(f)	1.16	2.18	0.01
(g)	1.31	2.46	0.27
(h)	1.49	4.18	0.91

Table 4.6: Corresponding to Figure 4.18

method is ranked first for the metric-based evaluation and last for the psychometric-based one.

(a) Original

(b) McCann99

(c) ACE

(d) Gibson

(e) Tarel

(f) DCP

(g) STRESS

(h) Ours

Figure 4.20: Gjøvik 3. Image taken in Gjøvik in winter 2014-2015.

Figure 4.20	e	$\bar{\gamma}$	σ
(b)	0.44	1.24	0
(c)	1.71	2.09	0.0002
(d)	1.78	2.11	0.03
(e)	3.13	2.98	0
(f)	1.74	1.96	0.01
(g)	1.65	2.04	0.29
(h)	1.83	3.91	1.04

Table 4.7: Corresponding to Figure 4.20

For this case, as we can see on the Table 4.7, our method has a good score with the first two parameters e and $\bar{\gamma}$ but still has trouble with the third one.

4.2 State of art images

Results we present here are from the first iteration of our application. Here we notice that our approach give an enhancement comparable to the state-of-the-art images even better sometimes. Above, we list the paper corresponding to each image.

- DC is the algorithm developed in [He et al., 2009].
- DC Fast is inspired from [He et al., 2010].
- Fattal is a new algorithm developed in [Fattal, 2014].
- Fattal 08 is the direction proposed in 2008 by Fattal.
- Kopf is proposed in [Kopf et al., 2008].
- Nishino is the approach developed in [Nishino et al., 2012].
- STRESS is a hybrid algorithm developed by Kolås, Farup, and Rizzi.
- Tan method is developed in [Tan, 2008].
- Tarel is a dehazing algorithm developed by Tarel and Hautière.
- Wiener is the classical Wiener filter for image restoration.

Figure 4.31 shows how can be efficient our approach for far objects.

(a) Original (b) DC (c) Fattal

(d) STRESS (e) STRESS (f) Ours

Figure 4.21: Original image from [Fattal, 2014]

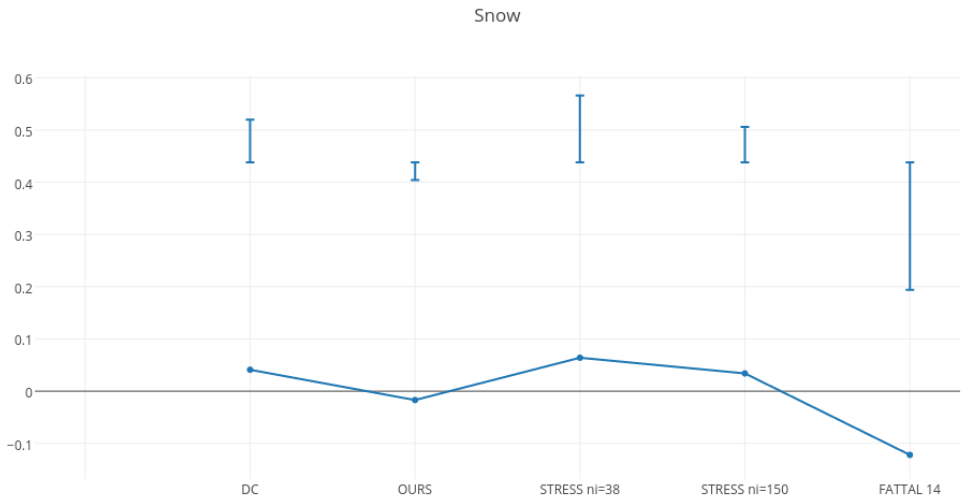

Figure 4.22: Psychophysical experiment for Snow.

Figure 4.21	e	$\bar{\gamma}$	σ
(b)	2.316	2.674	0.041
(c)	1.79	3.92	1.19
(d)	4.37	4.60	0.39
(e)	2.77	3.10	0.14
(f)	4.22	5.10	0.57

Table 4.8: Corresponding to Figure 4.21

In Figure 4.21, an example of a typical homogeneous hazy image, we can see how efficient is the dehazing processing by STRESS compare to two major approches [He et al., 2009] (DC) and Fattal color-lines concept [Fattal, 2014].

Setting the parameters $n_i = 150$ and $n_s = 5$ seems to be a good configuration for e and $\bar{\gamma}$ unlike σ. Setting $n_i = 38$ and $n_s = 20$, however are better for the score of the parameter σ. The best result for σ is given with the DCP (b). The psychometric-based evaluation shows that for our method the Z-score is very closed to zero and negative but still better than Fattal method, STRESS has the best subjective ranking.

(a) Original

(b) Wiener

(c) Nishino

(d) DC

(e) Fattal

(f) STRESS

(g) STRESS

(h) Ours

Figure 4.23: Original foggy image from [Nishino et al., 2012].

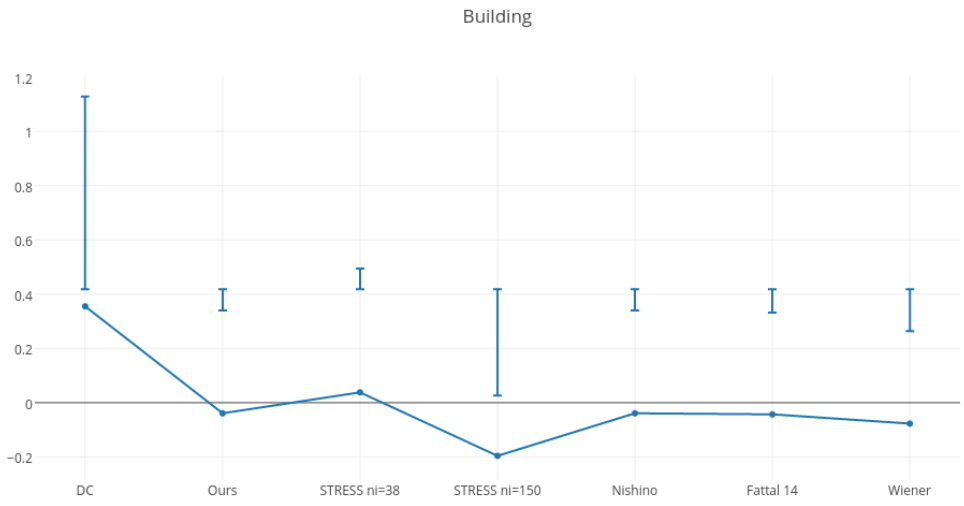

Figure 4.24: Psychophysical experiment for buildings.

In Figure 4.23, we have a smoothness issue on the boundaries of the building but still the visibility criterion is almost better than other cases.

STRESS based algorithms give best results for this series, as we can see on Table 4.9 on the last three lines. Nishino approach gives impressing result for e And $\bar{\gamma}$.

The psychometric image evaluation in Figure 4.24 shows that the lower band of the CI of all these algorithms, is negative. Two Z-score are positive: DC and STRESS with $n_i = 38$. Here we can see that there is no significant correspondence

Building	e	$\bar{\gamma}$	σ
(b)	−0.05	1.65	5.66
(c)	0.12	2.42	13.50
(d)	−0.03	2.31	2.60
(e)	−0.02	3.13	12.8
(f)	0.12	1.92	1.52
(g)	0.05	1.51	0.77
(h)	0.07	2.24	1.82

Table 4.9: Corresponding to Figure 4.23

between the metric-based evaluation and the psychometric evaluation except for STRESS with $n_i = 38$.

(a) Original

(b) Wiener

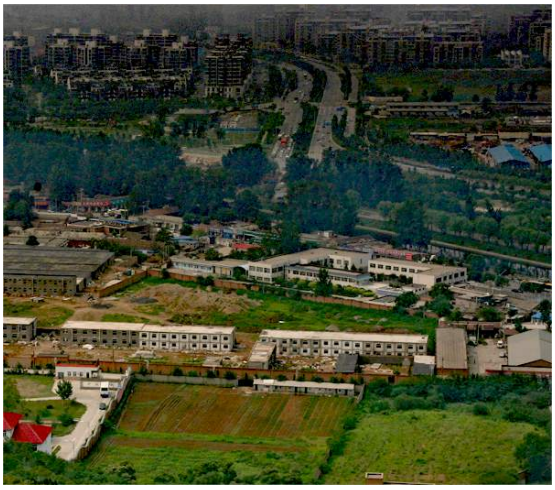

(c) Nishino

(d) DC

(e) Fattal

(f) STRESS

(g) STRESS (h) Ours

Figure 4.25: Original foggy image from [He et al., 2009].

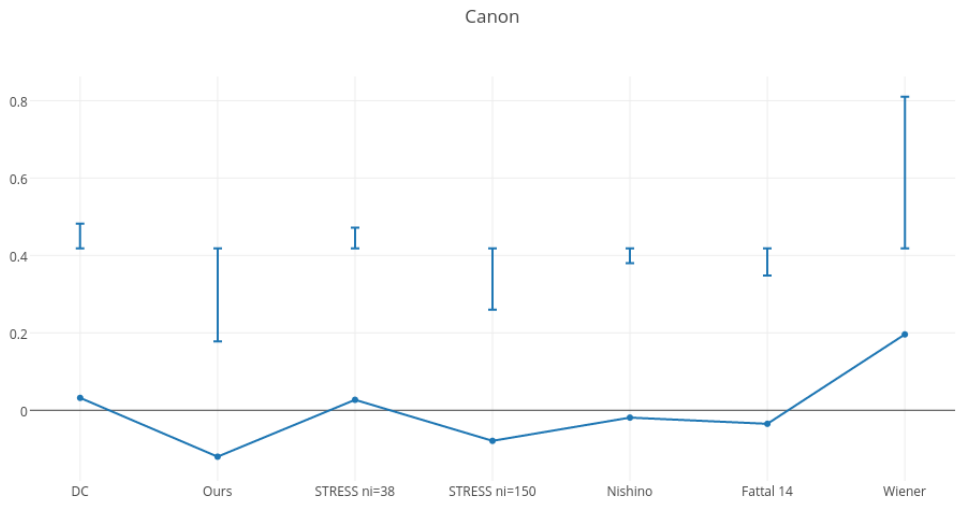

Figure 4.26: Psychophysical experiment for Canon.

In Figure 4.25, our output could be better for instance for a military application where the user would like to see clearly the details of objects but maybe less pleasing for TV application.

For this series on Table 4.10, Nishino, Fattal and ours gives the best result with the parameter e. For the second parameter $\bar{\gamma}$ we have respectively ours, Nishino

Figure 4.25	e	$\bar{\gamma}$	σ
(b)	2.26	5.07	0.004
(c)	3.78	8.24	21.18
(d)	3.02	6.43	1.23
(e)	3.44	6.29	21.87
(f)	3.32	4.68	0.31
(g)	2.83	3.57	0.09
(h)	3.44	8.32	0.50

Table 4.10: Corresponding to Figure 4.25

and the DCP which the best result. Wiener, STRESS and ours have the best scores. The psychometric evaluation seems to be good for Wiener, STRESS and DC. Our method gets the last ranking.

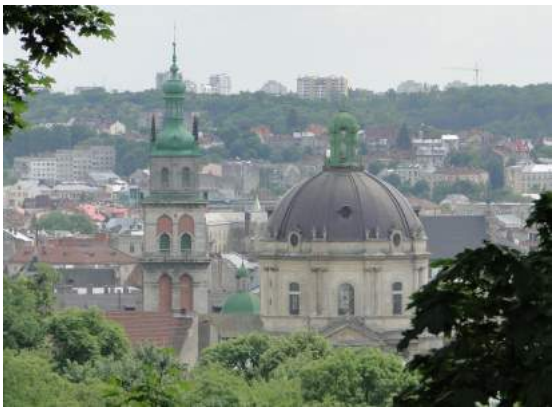

(a) Original

(b) DC

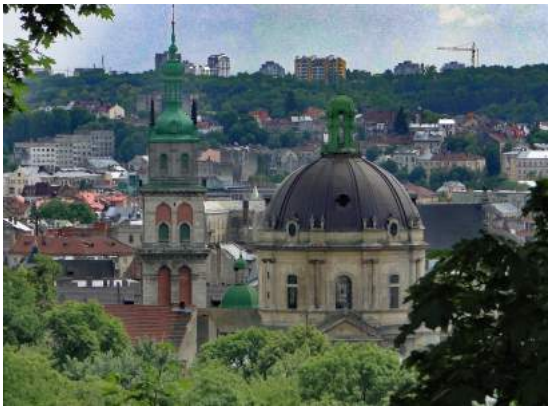

(c) DC Fast

(d) Fattal

(e) STRESS

(f) Ours

Figure 4.27: Original foggy image from [Fattal, 2014].

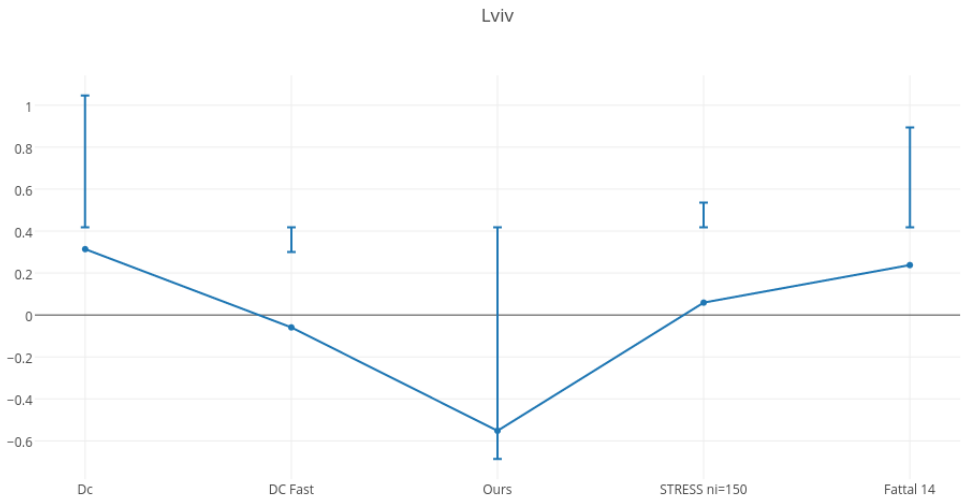

Figure 4.28: Psychophysical experiment for Lviv.

Figure 4.27	e	$\bar{\gamma}$	σ
(b)	0.21	3.27	1.73
(c)	0.41	2.83	0.06
(d)	0.25	1.52	0.02
(e)	0.40	1.87	1.92
(f)	0.34	2.13	2.22

Table 4.11: Corresponding to Figure 4.27

As you can see on Figures 4.27 and B.39[1], STRESS already removes fog from near objects. Our method here, processes also far objects.

Fattal has the best result for the last column of the Table 4.11. The best result for the second column are given by DCP and DC=Fast. The best result for the first column given by DC-Fast and STRESS.

Once again, for the subjective evaluation, our method has the last ranking with a large CI. The best result is given by DC, Fattal and STRESS which have positive Z-scores.

[1]see below.

(a) Original

(b) DC

(c) DC Fast

(d) Fattal

(e) STRESS

(f) Ours

Figure 4.29: Original foggy image from [He et al., 2009].

Ours has the third best score for the first and the third column of Table 4.12 and the best score for the second column

Figure B.39	e	$\bar{\gamma}$	σ
(b)	0.05	1.51	5.11
(c)	0.56	2.22	0.42
(d)	0.03	2.04	6.90
(e)	0.48	2.17	1.65
(f)	0.45	2.45	2.13

Table 4.12: Corresponding to Figure B.39

(a) Original (b) Fattal

(c) STRESS (d) Ours

Figure 4.30: Original foggy image from [Fattal, 2014].

The saturation effect that we have on Figure 4.30 does not look unpleasing. In that particular case, our algorithm fails to detect the sky.

On the above table, our method has clearly interesting score.

Figure 4.30	e	$\bar{\gamma}$	σ
(b)	−0.06	1.27	12.06
(c)	0.06	2.32	3.69
(d)	0.10	2.39	3.94

Table 4.13: Corresponding to Figure 4.30

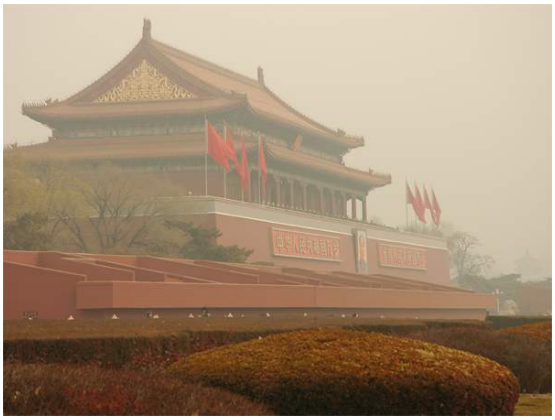

(a) Original

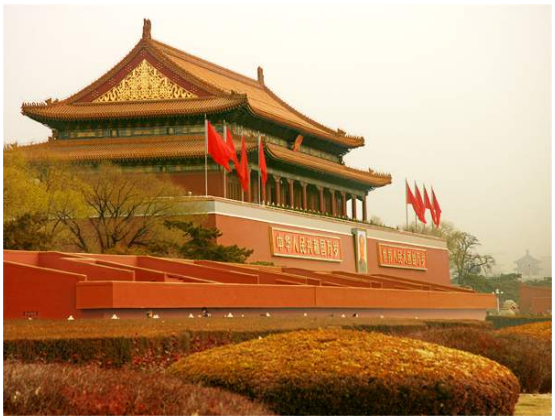

(b) DC

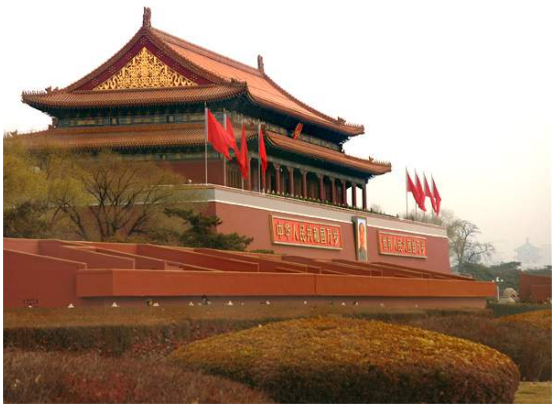

(c) Fattal

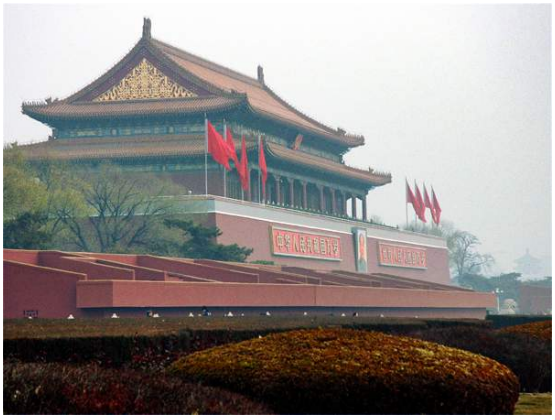

(d) STRESS

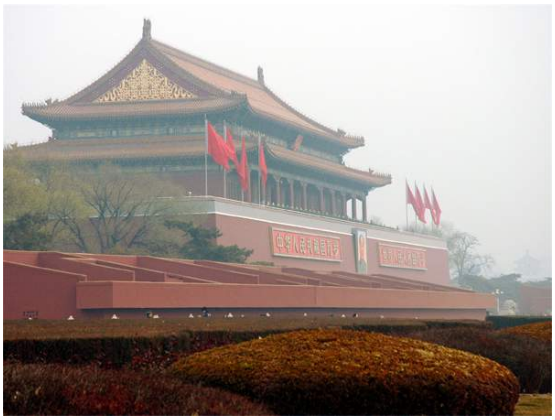

(e) STRESS

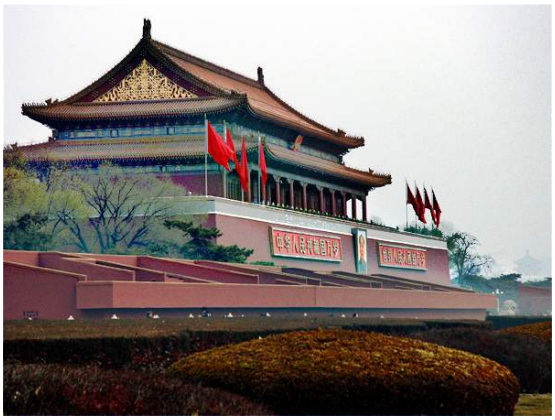

(f) Ours

Figure 4.31: Original foggy image from [He et al., 2009].

Figure 4.31	e	$\bar{\gamma}$	σ
(b)	0.37	2.38	1.54
(c)	0.40	1.95	0.26
(d)	0.64	1.17	1.96
(e)	0.45	1.59	0.60
(f)	0.57	2.43	1.37

Table 4.14: Corresponding to Figure 4.31

In Figure 4.31, we can see for instance a colour fidelity issue in our case, at the same time we have a good visibility in our method.

In the Table 4.14, we have impressive results with our method, as you can see with parameters e and $\bar{\gamma}$

(a) Original

(b) McCann99

4.3 failure case

(c) ACE

(d) Gibson

(e) Tarel

(f) DCP

(g) STRESS (h) Ours

Figure 4.32: NRK 3. Image courtesy NRK Sport Event.

In the Figure 4.32, our method seems to have a good visibility for object far away. One significant issue for this one is the colour of the snow on the background due to the fact that our algorithm processes the snow region by using the GDCP. The other issue is the colour fidelity. A formal labelling of the pixel can overcome this issue. We will see in Appendix B Section B.2, that the Remark 3.3.2 or the correlation between E^{max} and $E^{max}_{two\_scale\_STRESS}$ versus E^{min} and $E^{min}_{two\_scale\_STRESS}$ can be hold for a significant area of snow or sky region but not for small region.

5 Conclusion

We develop in this master thesis a new haze model and a new dehazing algorithm based on the STRESS framework closed to the classical one developed in the Equation 1.1. We also validate our new model theoretically and empirically. From this, we can say that the STRESS framework can be seen as a hybrid method since we know that STRESS solved also the Retinex problem.

In the first part of our work, we show that the STRESS framework can be seen as a good heuristics for the dehazing task as far as homogeneous (or dense) haze is taken into consideration [de Dravo and Hardeberg, 2015]. Futhermore, we demonstrate that we can identify a classical haze model parameters in Equation 1.2 with the new model derived from STRESS. As a consequence the estimation problem of the dehazing task falls into the state estimation of a given pixel: If the state of a pixel is well predicted, then we can apply the "good" scale for solving the defogging problem.

In the second part, we then model the outdoor hazy image in three regions which represent each, a stationnary problem in the sense of Hidden Markov Model (HMM) approach namely: near objects, far objects and sky region (and region similar to the sky region as snow region). These three regions can be seen as the state variables of our model sharing all, a common attribute: The radius parameter of the STRESS framework.

The radius parameter is crucial for the defogging problem and helps us to have a "good" assessment of the other parameters in the haze model that we develop. Therefore the airlight and the pseudo-transmission in our model are estimated in two ways. The first one consists of assessing these two parameters "globally" in the case of near objects and sky region. The second one falls in with the estimation of the parameters "locally" in the case of far objects.

To achieve the globality and the locality principles, we use the two-scale-STRESS by defining two different radius. Futhermore, these two radius are chosen in the way that we can have an aerial perspective in the image output. Even if, we have some case of failure, we show empirically that it is possible to overcome some colour fidelity case by having a formal labelling of the hazy image. We show that our method can be better than some of the state-of-the-art approaches in term of visibility and using the metrics defined in [Hautière et al., 2008].

In future work, we are planning to test our algorithms on more images including fog simulated in the context of indoor applications and also on video outdoor applications.

A Appendix A

In this appendix, we will briefly talk about identification systems which are the general expression of inverse problems. We will show a bit more in detail how STRESS is a valid estimator for the dehazing problem. We will begin by giving some interesting definitions. Sometimes, we will show the link between a given definition and the way the STRESS framework is built. Our presentation here is almost based on the book of Tangirala.

According to the same book, identification is the exercise of developing a mathematical relationship (model) between the causes (inputs) and the effects (outputs) of a system (process) based on observed or measured data. Stated otherwise, identification establishes a mathematical map between the input and output spaces as determined by the data.

With this definition in mind, we can see that both the forward and backward expression of the haze physical model deal with identification. Even if the model that we develop do not have a perfect matching with the classical haze model developed in Equation 1.1, we prove mathematically and empirically that our model is valid. In other hand, according to the author of the book, there are three facts of identification concerning the accuracy and precision of identified models:

- It is generally not possible to build an accurate model from finite-sample data
- It is generally not possible to estimate a precise model from finite-sample data
- The accuracy and precision of the optimally identified model, among other factors, is critically dependent on the (i) input type (excitation and shape, with the latter holding for non-linear systems) and the (ii) signal-to-noise ratio achieved in the experiment. A generalized term capturing both of these aspects is information. The quality of the final model depends on how informative the data is.

From these three facts and arguments that we develop in Section 1.6, neither the classical models of haze in Equations 1.1 and 1.2 nor ours in Equation 3.17 are accurate models of haze. So if we consider the Equation 3.17, how are we going to estimate or infer the unknowns. Before developing this process, let's talk about estimation.

According to [Tangirala, 2014]: Estimation is the exercise of methodically inferring the unobserved or hidden variable from a given information set using a mathematical map between the space of unknowns and knowns and a criterion for estimation. The device that performs the estimation is called the estimator.

We have two broad types of estimation problems: (1) signal estimation, (2) parameter estimation. In the recent years, a third category is added and corresponds to the state estimation. The latter also belongs to the family of signal estimation. Below, we give more details about these categories:

1. Signal estimation: Signals are usually available in the form of measurements that are contaminated by noise. The signal could be a regular 1-D signal, or a higher-dimensional variable such as an image. The goal is to estimate the signal(s) from the measurements. This class of estimation problems has lent itself to three sub-classes, namely, prediction, filtering and smoothing depending on the relative position of the sampling instant at which the estimate is desired with respect to the time horizon over which the data is available.
   - Prediction: The prediction problem, as the term implies, refers to the case when the information is available up to k and we are interested in estimating future values of the signal x[k + 1]; x[k + 2]; ...
   - Filtering: Filtering is concerned with the estimation of the signal at the kth (present) instant given information up to the k^{th} (present) instant. The Wiener filter, Kalman filter and particle filter are some examples.
   - Smoothing: smoothing is an estimation problem which relies on both past and future data to make an inference of the signal at the present instant.
2. Parameter estimation: The term parameter may either refer to a regression model parameter or the parameter of a probability distribution (density) function. In model parameter estimation, the form of the regression model is known and the user is interested in estimating the parameters of the model from the given data.
3. State estimation: As the name suggests, state estimation is concerned with the inference of states from given observations. The problem is naturally portrayed in the state-space framework and was largely popularized by [Kalman, 1960] in his seminar paper on Kalman filter.
   In our work, we also used a state estimation approach which allows us to know whether or not, a given pixel belongs to the sky region.

A.1 More details about STRESS and the dehazing task

In [Tangirala, 2014], the author considers the following forward model:

$$y[k] \quad = \quad c + e[k] \tag{A.1}$$

with $e[k] \sim WN(0, \sigma_e^2)$ and WN is a Gaussian white noise - or GWN. The problem is that we have N observations of $[y[k]]_{k=0}^{N-1}$ of a constant signal c, and we want to

obtain the "best" estimate of c. the parameters set from this problem is: $\theta = [c, \sigma_e^2]$ The solutions of this problem is given by the following equations:

$$\hat{c^\star} = \frac{1}{N}\sum_{i=0}^{N-1} y[k] \tag{A.2}$$

$$\hat{\sigma_e^2} = \frac{1}{N-1}\sum_{i=0}^{N-1} (y[k] - \hat{c^\star})^2 \tag{A.3}$$

From above equations $\hat{c^\star}$ (resp. $\hat{\sigma_e^2}$) is the optimum value of c (resp. of σ_e^2) derived from the following optimization problem in term of least squares estimation approach:

$$\min_\theta ||y - \hat{y}|| = \min_\theta \sum_{i=0}^{N-1} (y[k] - y[\hat{k}|\theta])^2 \tag{A.4}$$

The good news is that STRESS for the dehazing problem is doing almost the same process. In the following we will show how this is done in the STRESS framework by considering the Equation 3.17. Remember Theorem 3.2.1 and Corollary 3.2.1.1 that the goal is to be closed to the minimum envelope E^{min} for the dehazing task.

A.1.1 Estimating the airlight

As we demonstrate in Chapter 3, the airlight is represented by the variable $\bar{r}$ - see Equation 3.5 and is infered automatically in the framework. So when the radius is large, this parameter tends to be high and when the radius is small, the parameter is also not very large. Considering near objects and region similar to the sky, it seems from our experiment that the airlight should be high. For far objects, we notice the inverse phenomenon empirically.

A.1.2 estimating the transmission

Conjointly, we prove that the pseudo-transmission $\bar{w_2}$ is the complementary of $\bar{v}$ in the interval $[0, 1]$ and since we know that $p_{STRESS} = \bar{v}$, then the transmission can be thought as the inverse map of p_{STRESS}. This rough approximation of the transmission in the STRESS framework makes sense since we know about the

DCP: for near objects for instance, the pixel value will be low, taking an approximation of the inverse of p_{STRESS} as the transmission will make the transmission to be high.

A.1.3 Estimating the scene albedo

For the estimation of the albedo, let's consider the Equation 3.17. So if we want to get a similar form of 3.17 with Equation A.1, we should avoid multiplicative factor in our process.

$$\begin{aligned} I(x) &= J(x)t_1(x) + (1 - t_2(x))A(x) \qquad \text{(A.5)} \\ p_0 &= E^{min}\bar{w_1} + (1 - \bar{w_2})\bar{r} \\ p_0 &= E^{min} + (1 - \bar{w_2})\bar{r} \qquad \text{(A.6)} \end{aligned}$$

In Equation A.5, on the second line we have $\bar{w_1} = 1$. Let's assume that $\bar{r} \neq 0$, then we can divide the last expression by $\bar{r}$ and obtain the following relationship:

$$\begin{aligned} p_0 &= E^{min} + (1 - \bar{w_2})\bar{r} \qquad \text{(A.7)} \\ \frac{p_0}{\bar{r}} &= \frac{E^{min}}{\bar{r}} + \frac{(1 - \bar{w_2})\bar{r}}{\bar{r}} \\ \frac{p_0}{\bar{r}} &= \frac{E^{min}}{\bar{r}} + 1 - \bar{w_2} \\ \frac{p_0}{\bar{r}} &= \frac{E^{min}}{\bar{r}} + \bar{v} \qquad \text{(A.8)} \end{aligned}$$

Let's pose $\frac{p_0}{\bar{r}} = \bar{g}$ and $\frac{E^{min}}{\bar{r}} = \bar{g}$, so the above relationship can be written as follows:

$$\bar{g} = \bar{h} + \bar{v} \qquad \text{(A.9)}$$

The above relationship is quite similar to the one that we have in A.1 except the fact, in the right hand side, we do not have neither noise nor constant, so the parameter $\theta = [\sigma_h^2, \sigma_v^2]$. At this point, we can easily deduce how the albedo term corresponding to $\bar{v}$ is estimated[1].

[1] Again here, we should remember that the goal is to be near to the minimum envelope E^{min}.

B Appendix B

In this appendix, we will show more images that we process with our algorithm and some others. We will see that taking the envelope superior of the two-scale-STRESS can be critical for some images with snow. So to overcome this issue, we will develop in a second iteration a variant which allows us to improve a little bit the first iteration. .

B.1 Some images from the first iteration

(a) Original

(b) Tarel

(c) Nishino

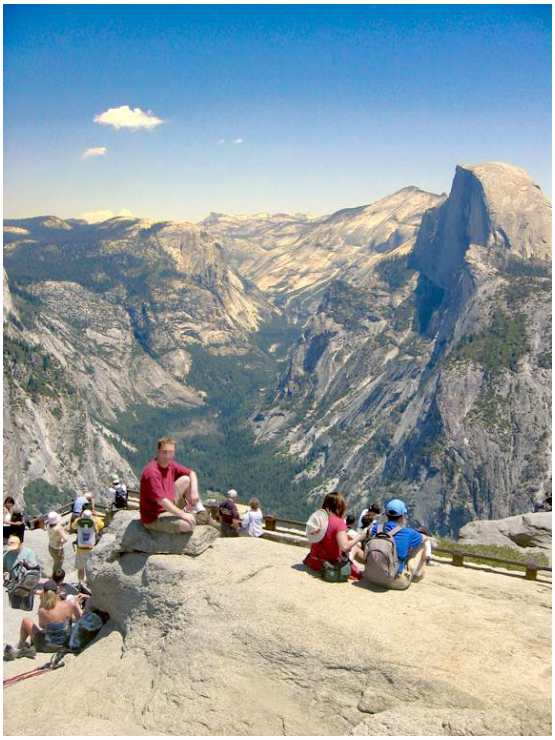

(d) DC

(e) Kopf

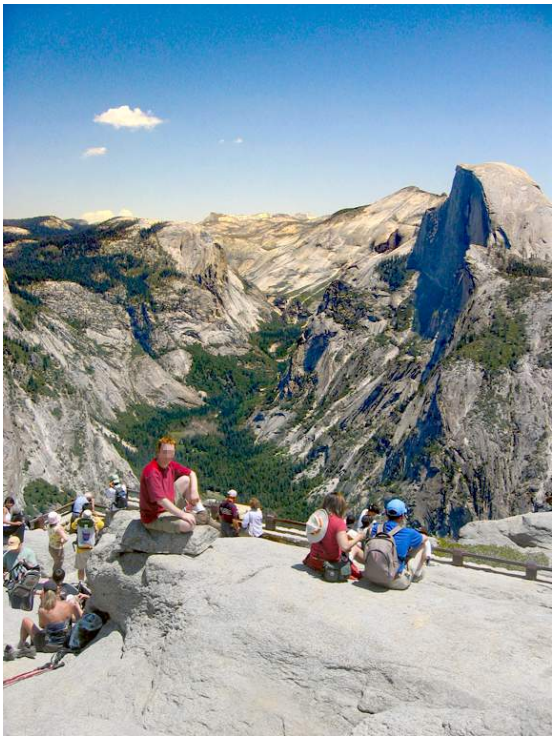

(f) Fattal

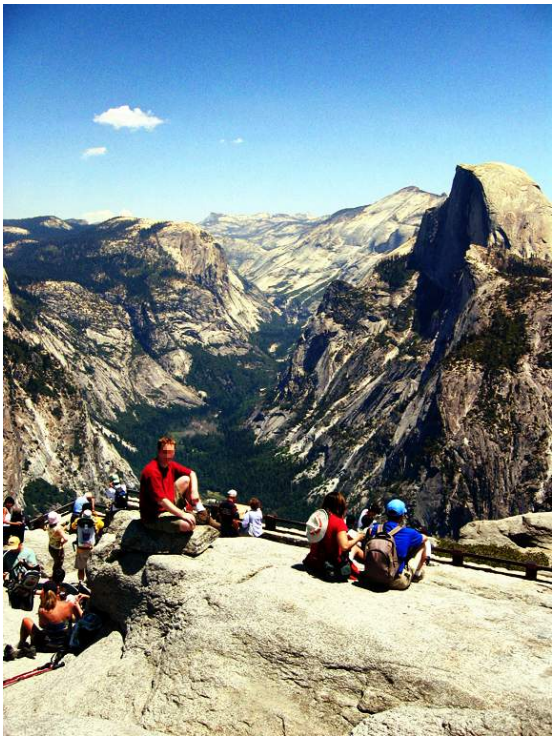

(g) STRESS

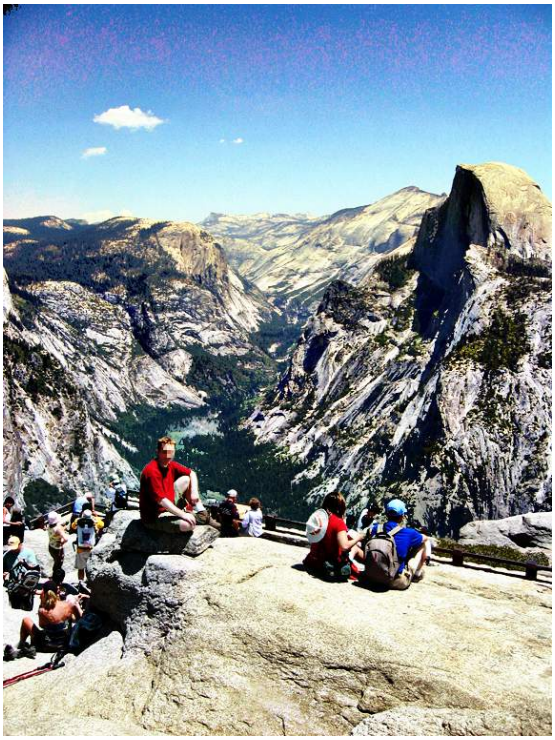

(h) Ours

Figure B.33: Original foggy image fromKopf et al. [2008].

Figure B.33	e	$\bar{\gamma}$	σ
(b)	0.66	2.32	0.03
(c)	0.18	1.52	11.07
(d)	0.17	1.76	1.83
(e)	0.12	1.33	1.59
(f)	0.03	2.16	3.16
(g)	0.39	2.10	0.73
(h)	0.38	3.05	0.96

Table B.15: Corresponding to Figure B.33

On Figure B.33, the haze on distant objects is well removed. However we get a saturation effect on the sky region, but this saturation effect does not look unnatural.

Once again, we can see on Table B.15, Tarel approach gives the best score for e parameter, ours often gives the best score for the parameter $\bar{r}$. Tarel, STRESS

and ours for the last parameter σ concede the best percentage.

(a) Original

(b) mcCann99

(c) DC

(d) Fattal 08

(e) Kopf

(f) Tan

(g) Tarel

(h) Fattal

(i) STRESS

(j) Ours

Figure B.34: Original foggy image from [Kopf et al., 2008].

Figure B.34	e	$\bar{r}$	σ
(b)	0.05	0.97	0.0002
(c)	−0.08	1.39	0.21
(d)	−0.04	1.34	2.60
(e)	0.004	1.37	1.16
(f)	0.007	5.40	1.83
(g)	0.06	2.02	0.008
(h)	0.02	1.97	5.56
(i)	0.07	1.70	0.70
(j)	−0.01	2.05	0.98

Table B.16: Corresponding to Figure B.34

The table B.16 shows that STRESS gives one of the best score with this image.

(a) Original

(b) McCann99

(c) ACE

(d) Schechner

(e) Fattal 08

(f) DCP

(g) Fattal 14

(h) STRESS

(i) Ours

Figure B.35: Description

(a) Original

(b) Fattal 08

(c) DC

(d) Fattal 14

(e) STRESS

(f) Ours

Figure B.36: Original foggy image from [He et al., 2009].

(a) Original

(b) DC

(c) Fattal 14

(d) STRESS

(e) STRESS

(f) Ours

Figure B.37: Original foggy image from [He et al., 2009].

(a) Original

(b) Wiener

(c) DC

(d) Fattal 14

(e) STRESS

(f) Ours

Figure B.38: Original foggy image from [He et al., 2009].

(a) Original

(b) Fattal 14

(c) STRESS

(d) Ours

Figure B.39: Original foggy image from [He et al., 2009].

B.2 Why the second iteration?

Applying the Remark 3.3.2 or the correlation between E^{max} and $E^{max}_{two\_scale\_STRESS}$ versus E^{min} and $E^{min}_{two\_scale\_STRESS}$[1] on a small area leads to the colour fidelity issues, as you can see on the Figure B.40. To overcome this issue, instead of applying the Remark 3.3.2 on pixels with high intensity value, we apply the STRESS framework with a radius $R = \max(w, h)$ or $R = \sqrt{w^2 + h^2}$.

[1]The Remark 3.3.2 is still valid but the correlation link is not anymore.

(a)original

(b)Iter 1

(c)Iter 2

Figure B.40: Gjøvik 4. In (b), we can see that the white color for a non-sky object looks unnatural. The reason is that the Remark 3.3.2 is only valid for sky region (and similar region). To overcome this issue, in (c), we apply the STRESS with a radius R for all pixels which have an intensity close to the intensity of pixels in the sky region. The goal again is to avoid a global labelling of the image which could be costly or critical.

B.3 Small sky area

As we said in Chapter 3, having in the image, a small area of sky region - for instance less than 50% of the total width of the image - leads to decide the abscence of sky region. One way to overcome this issue in our work is to implement the consecutivity criteria of a potential sky area. Figure B.41 shows clearly an example. The good news about our processing, is the fact that we can detect somehow this failure case. In fact, during tests of our algorithm, we trace the values which allow us to take decision about the presence or the abscence of a potential sky region. We noticed that, for the image on Figure B.41, we have many trips (here the marjority) with pixels intensities less than 60 - before meeting the first edge. At this step, we could design a voting algorithm which could discard these trips and update the total width to consider as a potential sky area. So the

(d) OUrs

Figure B.41: In (a) because our algorithm fails to detect the sky region, the sky looks saturated.

main issue with our method is a formal labelling - or a semantic issue - of the hazy image.

References

W. Adrian. Visibility of targets: Model for calculation. *Lighting Research and Technology*, 21(4):181–188, 1989. 2

R. Ajaj, N. Delprat, and C. Jacquemin. Journée d'étude STMA, BétonSalon, Paris, 2009. 1

A.C. Aponso and N. Krishnarajah. Review on state of art image enhancement and restoration methods for a vision based driver assistance system. with de-weathering. *Soft Computing and Pattern Recognition (SoCPaR)*, pages 135–140, Oct 2011. 1

M.R. Banham and A.K. Katsaggelos. Digital image restoration. *Signal Processing Magazine, IEEE*, 14(2):24–41, Mar 1997. ISSN 1053-5888. 7

Aurélien Bellet, Amaury Habrard, Emilie Morvant, and Marc Sebban. Learning A Priori Constrained Weighted Majority Votes. *Machine Learning*, 97(1-2): 129–154, 2014. 49

Ya bing Zhu, Jun min Liu, and Ying guang Hao. An single image dehazing algorithm using sky detection and segmentation. In *Image and Signal Processing (CISP), 2014 7th International Congress on*, pages 248–252, Oct 2014. doi: 10.1109/CISP.2014.7003786. 20

M. Born and E. Wolf. *Principle of Optics*. Pergamon, Oxford, 7th Edition., 1999. 6

Britannica. Aerial perspective. *home page on the Internet*, 2015. 1

John Canny. A computational approach to edge detection. *Pattern Analysis and Machine Intelligence, IEEE Transactions on*, PAMI-8(6):679–698, Nov 1986. ISSN 0162-8828. 43

P. Carr and R. Hartley. Improved single image dehazing using geometry. In *Digital Image Computing: Techniques and Applications, 2009. DICTA '09.*, pages 103–110, Dec 2009. 19

K.C. Chou, A.S. Willsky, A. Benveniste, and M. Basseville. Recursive and iterative estimation algorithms for multiresolution stochastic processes. In *Decision and Control, 1989., Proceedings of the 28th IEEE Conference on*, pages 1184–1189 vol.2, Dec 1989. 35

CIE. International lighting vocabulary. Cie technical report, CIE, 1987. 6

Kostadin Dabov, Alessandro Foi, Vladimir Katkovnik, and Karen Egiazarian. Image denoising by sparse 3d transform-domain collaborative filtering. *IEEE TRANS. IMAGE PROCESS*, 16(8):2080, 2007. 20

V. Whannou de Dravo and J.Y. Hardeberg. Stress for dehazing. In **Accepted* Colour and Visual Computing Symposium (CVCS)*, August 2015. 80

Hilda Deborah, Nol Richard, and Jon Yngve Hardeberg. Spectral ordering assessment using spectral median filters. In Jn Atli Benediktsson, Jocelyn Chanussot, Laurent Najman, and Hugues Talbot, editors, *Mathematical Morphology and Its Applications to Signal and Image Processing*, volume 9082 of *Lecture Notes in Computer Science*, pages 387–397. Springer International Publishing, 2015. ISBN 978-3-319-18719-8. doi: 10.1007/978-3-319-18720-4_33. 40

Zhi Dou, Yubing Han, Weixing Sheng, and Xiaofeng Ma. Image dehaze using alternating laplacian and beltrami regularizations. *Journal of Electronic Imaging*, 24(2):023004, 2015. 20

J. El Khoury, J.-B. Thomas, and A. Mansouri. Does dehazing model preserve color information? In *Signal-Image Technology and Internet-Based Systems (SITIS), 2014 Tenth International Conference on*, pages 606–613, Nov 2014. 3, 53

M. Elad. Retinex by two bilateral filters. *In Proceedings of Scale-Space*, pages 217 – 229, 2005. 11

P. Engeldrum. Psychometric Scaling: A Toolkit for Imaging Systems Development. 2000. 53

Xin Fan, Yi Wang, Renjie Gao, and Zhongxuan Luo. Haze editing with natural transmission. *The Visual Computer*, pages 1–11, 2015. ISSN 0178-2789. 20

Raanan Fattal. Single image dehazing. *ACM Trans. Graph.*, 27(3):72:1–72:9, August 2008. ISSN 0730-0301. iii, v, 2, 8, 13, 64

Raanan Fattal. Dehazing using color-lines. *ACM Trans. Graph.*, 34(1):13:1–13:14, December 2014. ISSN 0730-0301. iii, viii, 2, 14, 30, 64, 65, 72, 75

Paul Fieguth. *Statistical image processing and multidimensional modeling*. Information science and statistics. Springer, New York, 2011. ISBN 978-1-441-97293-4. 21, 35, 45

G. G. Field. Test image design guidelines for color quality evaluation. In *In Color Imaging Conference*, Scottsdale, AZ, USA, Nov 1999. 52

B. Funt, F. Ciurea, and J. Mccann. Retinex in matlab. In *Journal of Electronic Imaging*, pages 112–121, 2000. 51

D. Fussell. Ray tracing. *CS384G - Computer Graphics, University of Texas at Austin*, 2010. 6

A. Galdran, J. Vazquez-Corral, D. Pardo, and M. Bertalmío. A variational framework for single image dehazing. In **Accepted* in European Conference on Computer Vision Workshops*, 2014. v, 12

A.C. Gallagher, Jiebo Luo, and Wei Hao. Improved blue sky detection using polynomial model fit. In *Image Processing, 2004. ICIP '04. 2004 International Conference on*, volume 4, pages 2367–2370 Vol. 4, Oct 2004. 42

P. Getreuer. Automatic Color Enhancement (ACE) and its Fast Implementation. *Image Processing On Line*, 2:266–277, 2012. 51

K.B. Gibson and T.Q. Nguyen. On the effectiveness of the dark channel prior for single image dehazing by approximating with minimum volume ellipsoids. In *Acoustics, Speech and Signal Processing (ICASSP), 2011 IEEE International Conference on*, pages 1253–1256, May 2011. 19

K.B. Gibson, D.T. Vo, and Truong Q. Nguyen. An investigation of dehazing effects on image and video coding. *Image Processing, IEEE Transactions on*, 21(2):662–673, Feb 2012. 19, 51

K.B. Gibson, S.J. Belongie, and T. Q. Nguyen. Example based depth from fog. *Image Processing (ICIP), 2013 20th IEEE International Conference*, pages 728–732, Sept 2013. v, 1, 19, 26

Kristofor B. Gibson and Truong Q. Nguyen. An analysis of single image defogging methods using a color ellipsoid framework. *EURASIP J. Image and Video Processing*, 2013:37, 2013a. 19

Kristofor B. Gibson and Truong Q. Nguyen. Fast single image fog removal using the adaptive wiener filter. In *IEEE International Conference on Image Processing, ICIP 2013, Melbourne, Australia, September 15-18, 2013*, pages 714–718, 2013b. 19

A.S Glassner. *An introduction to ray tracing*. Morgan Kaufmann, 1989. 6

Christine Graffigne, Fabrice Heitz, Patrick Perez, Francoise J. Preteux, Marc Sigelle, and Josiane B. Zerubia. Hierarchical markov random field models applied to image analysis: a review, 1995. 35

D. Gutierrez, W. Jarosz, C. Donner, and S.G Narasimhan. Scattering. *in Proceeding SIGGRAPH 2009 ACM SIGGRAPH 2009 Course*, (21):1–14, Aug 2009. vii, 5, 6

Jacques Hadamard. *Lectures on Cauchy's problem in linear partial differential equations / Jacques S. Hadamard*. New Haven, 1923. 21

Kenneth M. Hanson. Introduction to Bayesian image analysis. volume 1898, pages 716–731. SPIE, 1993. 38

N. Hautière, J.-P. Tarel, D. Aubert, and E. Dumont. Blind contrast enhancement assessment by gradient ratioing at visible edges. *Image Analysis & Stereology Journal*, 27(2):87–95, 2008. iii, 2, 27, 80

K. He. *Single Image Haze Removal Using Dark Channel Prior*. PhD thesis, The Chinese University of Hong Kong, 2011. 16

K. He, J. Sun, and X. Tang. Single image haze removal using dark channel prior. *IEEE Conference on Computer Vision and Pattern Recognition (CVPR)*, pages 1956–1963, 2009. iii, v, viii, 2, 8, 10, 11, 12, 16, 19, 26, 30, 34, 42, 52, 64, 65, 70, 74, 77, 94, 95, 96, 97

K. He, J. Sun, and X. Tang. Guided image filtering. *The 11th European Conference on Computer Vision (ECCV)*, 2010. 64

Kaiming He, C. Rhemann, C. Rother, Xiaoou Tang, and Jian Sun. A global sampling method for alpha matting. In *Computer Vision and Pattern Recognition (CVPR), 2011 IEEE Conference on*, pages 2049–2056, June 2011. 31

M. Hébert. Ray scattering model for spherical transparent particles, 2013. 6, 7

ABM T. Islam and I. Farup. Spatio-temporal colour correction of strongly degraded movies. In *Color Imaging XVI: Displaying, Processing, Hardcopy, and Applications*, volume 7866 of *Proceedings of SPIE/IS&T Electronic Imaging*, page 78660Z, San Francisco, CA, USA, Jan 2011. SPIE. 24

ISO 204621:1994. *ISO 204621 photography psychophysical experimental methods to estimate image quality part 1: Overview of psychophysical elements*. ISO. 52

Pat S. Chavez Jr. An improved dark-object subtraction technique for atmospheric scattering correction of multispectral data. *Remote Sensing of Environment*, 24(3):459 – 479, 1988. ISSN 0034-4257. 19

Rudolph Emil Kalman. A new approach to linear filtering and prediction problems. *Transactions of the ASME–Journal of Basic Engineering*, 82(Series D): 35–45, 1960. 82

R Khan, D. Muselet, and A Trémeau. Texture classification across illumination color variations. In *International Journal of Computer Theory and Engineering*, volume 5, pages 65–70, 2013. 23

Andreas Kirsch. *An introduction to the mathematical theory of inverse problems*. Applied mathematical sciences. Springer, New York, 1996. ISBN 0-387-94530-X. 22

Ø. Kolås, I. Farup, and A. Rizzi. Spatio-temporal retinex-inspired envelope with stochastic sampling: a framework for spatial color algorithms. *Journal of Imaging Science and Technology*, 55(4):040503–1–040503–10, 2011. iii, 1, 24, 25, 29, 30, 31, 64

Johannes Kopf, Boris Neubert, Billy Chen, Michael F. Cohen, Daniel Cohen-Or, Oliver Deussen, Matt Uyttendaele, and Dani Lischinski. Deep photo: Model-based photograph enhancement and viewing. *ACM Transactions on Graphics (Proceedings of SIGGRAPH Asia 2008)*, 27(5):116:1–116:10, 2008. viii, 9, 64, 88, 92

H. Koschmieder. Theorie der horizontalen sichtweite. *In Beitr. zur Phys. d. freien Atm*, page 171181, 1924. 7, 21

L. Kratz and K. Nishino. Factorizing scene albedo and depth from a single foggy image. In *Computer Vision, 2009 IEEE 12th International Conference on*, pages 1701–1708, Sept 2009. v, 19, 35

R. L. Lagendijk and J. Biemond. In Jerry D. Gibson and Al Bovik, editors, *Handbook of Image and Video Processing*. 2000. 7

A. Levin, D. Lischinski, and Y. Weiss. A closed-form solution to natural image matting. *Pattern Analysis and Machine Intelligence, IEEE Transactions on*, 30(2):228–242, Feb 2008. ISSN 0162-8828. 17

X. Liu and J.Y Hardeberg. Fog removal algorithms : a survey and perceptual evaluation. *European Workshop on Visual Information Processing (EUVIP) Paris, France*, June 2013. 2, 20

Lennart Ljung, editor. *System Identification (2Nd Ed.): Theory for the User*. Prentice Hall PTR, Upper Saddle River, NJ, USA, 1999. ISBN 0-13-656695-2. 21

C.H Major and M.S Baden. *An introduction to quantitative research synthesis: Managing the information explosing in social science*. Routledge, 2010. 3

Erik Matlin and Peyman Milanfar. Removal of haze and noise from a single image, 2012. 20

E. J. McCartney. *Optics of the Atmostphere*. John Wiley, New York. 4

Kenney Mencher. Perspective. *home page on the Internet*, 2015. 1

M.I Mishchenko, L.D. Travis, and A.A. Lacis. *Optical models for color reproduction*. NASA Goddard Institute for Space Studies, 2005. 7

S.G Narasimhan and S.K Nayar. Vision and the atmosphere. *International Journal of Computer Vision*, 48(3):233254, 2001. 1, 4, 9, 20

S.G Narasimhan and S.K Nayar. Contrast restoration of weather degraded image. *Pattern Analysis and Machine Intelligence, IEEE Transactions on*, 25(6): 713724, June 2003. ISSN 0162-8828. 1, 8, 9, 20

Ko Nishino, Louis Kratz, and Stephen Lombardi. Bayesian defogging. *Int. J. Comput. Vision*, 98(3):263–278, July 2012. ISSN 0920-5691. v, viii, 19, 35, 64, 67

J.P. Oakley and Hong Bu. Correction of simple contrast loss in color images. *Image Processing, IEEE Transactions on*, 16(2):511–522, Feb 2007. ISSN 1057-7149. 19

Patrick Perez. Markov random fields and images. *CWI Quarterly*, pages 413–437, 1998. 39

E. Provenzi, M. Fierro, A. Rizzi, L. De Carli, D. Gadia, and D. Marini. Random spray retinex: A new retinex implementation to investigate the local properties of the model. *Trans. Img. Proc.*, 16(1):162–171, January 2007. ISSN 1057-7149. 24, 25

P. Sa. *Light transport in tissues*. PhD thesis, University of Texas, 1988. [PHD Thesis]. 6

Y.Y. Schechner, S.G. Narasimhan, and S.K. Nayar. Instant dehazing of images using polarization. In *Computer Vision and Pattern Recognition, 2001. CVPR 2001. Proceedings of the 2001 IEEE Computer Society Conference on*, volume 1, pages I–325–I–332 vol.1, 2001. 20

D. Shaked and R. Keshet. Robust recursive envelope operators for fast retinex. Technical report, HP Laboratories Israel, Technion City, Haifa 32000, Israel (2004), 2002. 24

S. Shwartz, E. Namer, and Y.Y. Schechner. Blind haze separation. In *Computer Vision and Pattern Recognition, 2006 IEEE Computer Society Conference on*, volume 2, pages 1984–1991, 2006. 20

G. Simone and I. Farup. Spatio-temporal retinex-like envelope with total variation. In *6th European Conference on Colour in Graphics, Imaging, and Vision (CGIV)*, pages 176–181, Amsterdam, Netherland, May 2012. 24

G. Simone, M. Pedersen, and J.Y. Hardeberg. Measuring perceptual contrast in uncontrolled environments. In *Visual Information Processing (EUVIP), 2010 2nd European Workshop on*, pages 102–107, July 2010. doi: 10.1109/EUVIP.2010.5699114. 53

L. Simonot, M. Hébert, R.D. Hersch, and H. Garay. Ray scattering model for spherical transparent particles. *Journal of Optical Society of America A, (JOSA A)*, 25(7):1521–1534, 2008. 6, 7

Iris Sprow, Zofia Baranczuk, Tobias Stamm, and Peter Zolliker. Web-based psychometric evaluation of image quality, 2009. 53

R.T Tan. Visibility in bad weather from a single image. *Proceeding of IEEE CVPR*, 2008. v, 8, 15, 29, 64

K. Arun Tangirala. *Principles of System Identification: Theory and Practice*. CRC Press, 2014. 81, 82

J-P. Tarel and N. Hautière. Fast visibility restoration from a single color or gray level image. In *Proceedings of IEEE International Conference on Computer Vision (ICCV'09)*, pages 2201–2208, Kyoto, Japan, 2009. v, 8, 18, 52, 55, 64

H. Tsutsui, S. Yoshikawa, H. Okuhata, and T. Onoye. Halo artifacts reduction method for variational based realtime retinex image enhancement. *Signal & Information Processing Association Annual Summit and Conference (APSIPA ASC)Asia-Pacific, Hollywood, CA*, 2012. 10

W. Wang and L. Xu. Retinex algorithm on changing scales for haze removal with depth map. *International Journal of Hybrid Information Technology*, 7 (4):353–364, 2014. v, 1, 10

Norbert Wiener. *Extrapolation, interpolation, and smoothing of stationary time series : with engineering applications*. M.I. T. paperback series. Cambridge, Mass. Technology Press of the Massachusetts Institute of Technology, 1964. First published during the war as a classified report to Section D2, National Defense Research Committee. 64

Wikipedia. Aerosol. *Wikipedia, the free encyclopedia*, December 2014. 4

Wikipedia. Mie scattering. *Wikipedia, the free encyclopedia*, Jan 2015a. 7

Wikipedia. Aerosol. *Wikipedia, the free encyclopedia*, January 2015b. 6

Wikipedia. Continuous function — Wikipedia, the free encyclopedia, 2015c. [Online; accessed 9-January-2015]. 22

B. Xie, F. Guo, and Z. Cai. Improved single image dehazing using dark channel prior and multi-scale retinex. In *Proceedings of the 2010 International Conference on Intelligent System Design and Engineering Application*, pages 848–851, October 13-14 2010. v, 9, 11, 12

G. Yadav, S. Maheshwari, and A. Agarwal. Fog removal techniques from images: A comparative review and future directions. *Signal Propagation and Computer Technology (ICSPCT), 2014 International Conference*, pages 44 – 52, Jul 2014. 1

H. Zhang, Q. Liu, F. Yang, and Y. Wu. Single image dehazing combining physics model based and non-physics model based methods. *Journal of Computational Information Systems*, 9(4):1623–1631, 2013. v, 9, 10, 11, 12

R. Zhang. Getting to the critical nucleus of aerosol format. *Science*, 328(5984): 1366–1367, June 2010. 4